Master's Thesis

for the achievement of the academic degree

Diplom-Ingenieur

in the field of study Energy Systems and Automation Technology
at TU Wien

Potential savings on investments for fast-charging infrastructure by spatio-temporal coordination of charging processes for long-distance passenger car trips

submitted at
Institute of Energy Systems and Electrical Drives

Supervisor: Associate Prof. Dipl.-Ing. Dr.techn. Johann Auer
Assistent: Dipl-Ing. Antonia Golab

by

Julius Ralf Friedrich
12027480

Vienna, March 2025

Statutory Declaration

I declare that I have authored this thesis independently, that I have not used other than the declared sources/resources, and that I have explicitly marked all material which has been quoted either literally or by content from the used sources.

Wien, ______________________ ______________________

Date Signature

Eidesstattliche Erklärung

Ich erkläre an Eides statt, dass ich die vorliegende Arbeit selbstständig verfasst, andere als die angegebenen Quellen/Hilfsmittel nicht benutzt, und die den benutzten Quellen wörtlich und inhaltlich entnommenen Stellen als solche kenntlich gemacht habe.

Wien, am ______________________ ______________________

Datum Unterschrift

Abstract

The transport sector is one of the largest emitters of CO_2 emissions and therefore represents a key challenge for achieving national and international climate targets. The increasing spread of battery electric vehicles requires an efficient use of the existing fast charging infrastructure, especially on highly frequented traffic routes such as highways. In this thesis, a mathematical optimisation model based on the bottom-up method is further developed. The aim of the model is to identify unused capacities of fast-charging stations through various expansion stages of charging coordination and to generate potential savings in fast-charging infrastructure investments. The study is based on Austrian traffic data, with the A2 highway serving as the case study region. Two vehicle categories are defined in this model: One category represents vehicles that participate in charging coordination, while the other category represents vehicles that do not participate in charging coordination. The optimisation takes into account various scenarios, such as the number of vehicles considered as well as traffic changes due to the weekend and seasonal tourist traffic. The results show that a significant increase in the efficiency of fast-charging capacity utilisation can be achieved by coordinating the charging processes. Furthermore, it becomes clear that charging coordination contributes to a smoother distribution of charging processes and charging capacity across different locations and could thus reduce local demand peaks. In addition, charging coordination can better mitigate seasonal traffic fluctuations and increased traffic density at weekends, which contributes to a more efficient utilisation of the existing infrastructure and enables more precise planning of fast-charging infrastructure requirements. The effectiveness of charging coordination depends largely on the number of vehicles taken into account, as a larger number of vehicles enables a more balanced distribution of charging processes. Charging coordination therefore helps to reduce investment costs in new charging points.

Kurzfassung

Der Transportsektor ist einer der größten Verursacher von CO2-Emissionen und stellt somit eine zentrale Herausforderung für die Erreichung nationaler und internationaler Klimaziele dar. Die zunehmende Verbreitung von Batterie-Elektrofahrzeugen erfordert eine effiziente Nutzung der bestehenden Schnellladeinfrastruktur, insbesondere auf hochfrequentierten Verkehrswegen wie Autobahnen. In dieser Arbeit wird ein mathematisches Optimierungsmodell weiterentwickelt, das auf der Bottom-up-Methode basiert. Ziel des Modells ist, die Identifizierung ungenutzter Kapazitäten von Schnellladestationen durch verschiedene Ausbaustufen einer Ladekoordination zu identifizieren und daraus ein Einsparungspotenzial an Schnellladeinfrastruktursinvestitionen zu generieren. Die Untersuchung erfolgt anhand von österreichischen Verkehrsdaten, wobei die Autobahn A2 als Fallstudienregion dient. In diesem Modell werden zwei Fahrzeugkategorien definiert: Die eine Kategorie repräsentiert die Fahrzeuge, welche an einer Ladekoordination teilnehmen, während die andere Kategorie Fahrzeuge repräsentiert, welche nicht an einer Ladekoordination teilnehmen. Die Optimierung berücksichtigt verschiedene Szenarien, wie die Anzahl der betrachteten Fahrzeuge sowie die Verkehrsveränderungen durch das Wochenende und durch saisonellen Tourismus Verkehr. Die Ergebnisse zeigen, dass durch eine Ladekoordination der Ladevorgänge eine signifikante Effizienzsteigerung der Schnellladekapazitätsnutzung erzielt werden kann. Darüber hinaus wird deutlich, dass Ladekoordination zur gleichmäßigeren Verteilung der Ladevorgänge und Ladeleistung auf verschiedene Standorte beiträgt und dadurch lokale Überlastungen reduzieren könnte. Darüber hinaus kann eine Ladekoordination saisonale Verkehrsschwankungen und erhöhte Verkehrsdichten an Wochenenden besser abfedern, was zu einer effizienten Nutzung der vorhandenen Infrastruktur beiträgt und ermöglicht eine präzisere Planung des Schnellladeinfrastrukturbedarfs. Die Effektivität der Ladekoordination hängt maßgeblich von der Anzahl der berücksichtigten Fahrzeuge ab, da eine größere Fahrzeugmenge eine gleichmäßigere Verteilung der Ladevorgänge ermöglicht. Die Ladekoordination trägt somit dazu bei, Investitionskosten in neue Ladepunkte zu verringern.

Contents

List of Acronyms

ASFINAG	Autobahnen- und Schnellstraßen-Finanzierungs-Aktiengesellschaft
BEV	Battery Electric Vehicle
CO_2	Carbon Dioxide
CS	Charging Station
CTR	Controlled
EU	European Union
GHG	Greenhouse Gas
POI	Point of Interest
RND	Random
SOC	State of Charge
UN	United Nations
V2G	Vehicle to Grid

List of Figures

List of Tables

1 Introduction

1.1 Motivation

Increasing public awareness of climate change is leading to greater demand for environmentally friendly mobility options. Battery electric vehicles (BEVs) are seen as a crucial factor in reducing Carbon Dioxide (CO_2) emissions and complying with the Paris Agreement [1]. The Paris Agreement commits the signatory states to drastically reduce their CO_2 emissions. The overarching goal of the 196 parties at the United Nations (UN) Climate Change Conference is to keep the increase in global average temperature to well below 2°C above pre-industrial levels and to pursue efforts to limit the temperature increase to 1.5°C above pre-industrial levels [2]. The transport sector, as one of the main emitters of greenhouse gases, is a particular focus of attention. In 2022, nearly 24 percent of greenhouse gases in the European Union (EU) will be attributable to the domestic transport sector [3]. In Austria, the transport sector is responsible for a large proportion of greenhouse gases [4]. The implementation of intelligent charging coordination can support compliance with climate targets by helping to maximize the use of renewable energy in road transport. More efficient use of charging infrastructure can also reduce the construction of new fast-charging stations, which minimizes land consumption and environmental impact.

The increasing popularity of BEVs requires an efficient and sust ainable charging infrastructure, especially on highways, to enable long-distance driving. As the market share of BEVs in Austria is steadily increasing, strategic charging coordination is essential to avoid charging bottlenecks, avoid unnecessary burden on the electricity grid and make optimal use of the existing fast-charging infrastructure. BEV registrations in Austria are rising continuously, which increases the demand for charging infrastructure on freeways. At the end of December 2024, Austria had 200,603 battery electric vehicles [5]. Forecasts assume that the share of BEVs will continue to grow in the coming years. A global market volume of EUR 986.8 billion is forecast for 2029, which corresponds to expected annual sales growth of almost 7 percent in the years 2025 to 2029 [6]. This poses a challenge for the charging infrastructure and energy management, as there is only limited connection capacity to the power grid.

The expansion of the charging infrastructure is a crucial factor in the nationwide spread of electromobility and requires needs-based planning and considerable investment. Efficient use of the expanded charging capacities is essential in order to avoid high investment costs for further infrastructure measures. A key challenge is to provide sufficient charging points in both the public and private sectors in order to minimise range anxiety [7] and ensure an even load on the grid. In addition, regulatory hurdles, grid expansion requirements and economic aspects must be taken into account in order to ensure a sustainable, efficient and user-friendly charging infrastructure.

Charging coordination for BEVs describes the intelligent control of the charging process in order to utilise the limited resources of the electricity grid efficiently and avoid bottlenecks. It comprises two central dimensions: a temporal and a spatial dimension. The temporal dimension relates to the question of when a vehicle is charged in order to reduce peak loads. The spatial dimension, on the other hand, addresses where charging takes place, for example through the intelligent distribution of vehicles to different charging points or charging zones. Coordinated charging coordination can ensure grid stability [8], reduce waiting times and utilise the charging infrastructure more efficiently. Such a system can be designed both centrally, by grid operators or aggregators, and decentrally, by vehicle users and charging providers.

1.2 Research questions

The increase in the number of BEVs sold require optimal use of existing capacities and minimization of the burden on the grid due to an excessive number of fast-charging stations. A suitable method for overcoming these challenges is spatio-temporal charging coordination, which enables optimal use of the existing infrastructure while ensuring sufficient charging infrastructure. This study therefore addresses two research questions.

1. How much cost savings due to reduced fast-charging capacity needs can be achieved by coordinating charging processes of battery electric vehicles (BEVs) along a highway network?
2. How are these cost savings affected by different conditions in charging demand patterns due to variations in outdoor temperature and traffic flow?

Traffic data from Austria is used to evaluate the impact of introducing charging coordination in various expansion stages. The aim of the study is to determine the potential capacity savings and cost savings. Another subject of the study is the influence of charging coordination on the required capacity under extreme traffic and temperature situations.

2 State of the art

This chapter provides an overview of the current state of research in the field of electromobility. Firstly, the transport sector and its influence on greenhouse gas emissions are considered in order to illustrate the need for a sustainable transformation. It then looks at the electrification of road transport. The expansion of the fast-charging infrastructure is discussed, as this plays a decisive role in the acceptance and practicality of electric mobility. Then, it also analyses how various charging coordination strategies already optimize the operation of BEVs and reduce grid loads. Finally, the contribution of this thesis is presented.

2.1 Electrification of the Austrian passenger car fleet

The transport sector is responsible for a significant share of greenhouse gas emissions. In Austria, the transport sector recorded total emissions of 29.9 million tonnes of CO2 equivalent in 2023, which corresponds to 44.8 percent of the country's total emissions. This makes transport the largest emissions sector in Austria. The percentage distribution of greenhouse gas emissions across the various sectors in Austria in 2023 is shown in Table 2.1 [4]. With almost 70 million tonnes of CO2 equivalent, Austria ranks 10th among the countries with the highest emission levels in the EU [3]. With a population of 9.16 million people in 2024, Austria is the 14th most populous country in the EU [9]. The majority of emissions in the transport sector are attributable to passenger and commercial transport [10]. A downward trend in Greenhouse Gas (GHG) emissions in Austria has been recognisable since 2005, but further emission reductions are necessary in order to achieve the goals of the Paris Agreement [2]. The transport sector is the second largest sector after the building sector in terms of changes in GHG-emissions between 2005 and 2023. The transport sector recorded a decrease in emissions of almost 5 million tonnes of CO2 equivalent compared to 2005, although the number of vehicles has increased [4]. In 2005, the number of motor vehicles in Austria was 5.6 million, while in 2023 it was around 7.3 million [11]. With 155,490 BEVs in Austria in 2023, this corresponds to just over 2 percent of the total number of vehicles in Austria [[5]. In 2013, the number of BEVs in Austria totalled just 2,070 [12]. The increasing number of motor vehicles and the simultaneous reduction in emissions show on the one hand that modern vehicles have lower emissions when travelling and on the other that the introduction of BEVs has a positive impact on GHG emissions.

Sector	Percentage share of GHG emissions in AT in 2023
Transport	44,8 %
Agriculture	19,3 %
Building	14,3 %
Energy and industry	12,4 %
Waste management	5,1 %
Fluorinated gases	4,1 %

Table 2.1: Share of sectors in total GHG emissions in AT in 2023

The study by Priessner et al. [13] analyses the factors that influence the acceptance and spread of BEVs in Austria. Although obstacles such as purchase price and range anxiety are decreasing, the growth in sales of BEVs is still lagging behind industry expectations. The authors analyse which psychological, socio-demographic and political framework conditions play a role in developing more targeted incentive measures to promote electric mobility. Based on a representative survey in Austria, they segment potential buyers into different groups and assess their attitudes towards purchase incentives. The study shows that environmental awareness and an affinity for technology are decisive factors for the early acceptance of BEVs, while a more individualistic attitude and scepticism towards new technologies inhibit acceptance. It also shows that people in regions with political incentives tend to favour BEVs.

2.2 Fast-charging infrastructure planning and expansion

The increase in the number of BEVs is directly linked to the expansion of the fast-charging infrastructure. While 10,442 public charging points were available in Austria in 2021, there were already 25,236 public charging points in 2024 [5]. In the Austrian capital Vienna, 2,845 public charging points were recorded in 2024. In addition to the expansion of public transport and cycling infrastructure, the electrification of transport in Vienna is an absolute necessity, as the city's climate goal is to reduce CO_2 emissions in the transport sector to zero by 2024 [14].

A study conducted in 2022 by Paul Pfaffenbichler [15] concludes that a number of 377,000 to 454,000 registered BEVs can be expected in Vienna in 2040. However, in order for electromobility to achieve a breakthrough, an appropriate infrastructure is required. This study is dedicated to the question of what the public charging infrastructure would need to look like in order to meet future energy requirements. For this purpose, four different scenarios for the ramp-up curves for BEVs and charging stations up to the year 2040 are considered.

The paper by Ullah et al. [16] investigates how to optimise the location of fast-charging stations to ensure efficient use and promote the acceptance of BEVs. The authors analyse the location of existing charging stations in Aichi Prefecture, Japan, and develop a model for the optimal placement of new fast charging stations. They consider various factors such as the range of the vehicles, investment costs and convenience for users. The model is based on five linear optimization models and a weighted set-covering method to determine both the number and locations of charging stations. The results show that strategic placement of charging stations improves charging accessibility and is economically viable. The study provides valuable insights for policy makers to support efficient investments in fast charging infrastructure.

2.3 Charging coordination approaches

However, as the increasing number of BEVs on the grid also has a detrimental effect on the supply network, the work by Corinaldesi et al. [1] analyses the economic impact of different charging strategies for BEVs in an Austrian office location. The aim is to optimize the costs of vehicle charging and minimise the negative effects on the electricity grid. To this end, a mathematical model was developed that solves various optimization problems for different charging strategies. The study analyses four different strategies and carries out sensitivity analyses and shows that optimized control of the charging process can lead to a reduction in costs. In addition, the financial advantage of such control increases when grid-related electricity prices rise. The methodology is based on linear optimization models and real measurement data to validate the approaches.

The work by Diaz-Londono et al. [17] analyses various strategies for the coordinated integration of BEV charging infrastructures into the electricity grid with transformer limits. The main problem is that uncoordinated charging can lead to grid congestion, especially at peak times. The authors compare three approaches: uncoordinated standard charging, a strategy that optimizes charging at times of low electricity prices and a strategy that aims for a more even load distribution in the grid. Simulations show that the second strategy leads to cost savings for users, while the third strategy minimises grid congestion. Both optimized methods can enable a more efficient integration of BEVs and ensure grid stability. The work uses mathematical optimization models and simulations to validate the effectiveness of the strategies.

A smart strategy for coordinated charging of BEVs in low-voltage grids is presented by Faghihi et al. [18]. The aim is to avoid grid congestion while minimising costs for users. To this end, BEVs are categorised into three priority groups: high priority (low state of charge), normal priority and low priority. Users receive different charging times with varying prices depending on the group. A load flow program checks the grid capacity before charging begins, and an optimization model minimises energy costs while complying with voltage and power limits. Simulations show that the model successfully performs load shifting and avoids grid bottlenecks without compromising users' mobility requirements.

Verbist et al. [19] analyse the effects of dynamic electricity tariffs on the charging of BEVs in low-voltage grids. Given the increasing number of EVs in distribution grids, smart charging is considered necessary to minimise grid reinforcements and avoid capacity problems. The authors develop an optimization model for public charging in a Dutch low-voltage grid that would be affected by overloads and voltage problems by 2050 without smart charging. The study compares different tariff models and finds that dynamic grid charges are superior to fixed tariffs as they promote better load balancing and reduce grid congestion. It also shows that bidirectional charging (Vehicle to Grid (V2G)) not only improves grid stability, but also reduces costs for operators while increasing BEV user satisfaction.

2.4 Own contribution

The optimization model presented in this paper builds on existing research results from Golab et al. and adds several new perspectives and analyses to the current state of the art. The work of Golab et al. presents a spatio-temporal model to identify potential bottlenecks in planned charging infrastructure for battery electric vehicles (BEVs) on highways by modelling charging activities based on traffic flows between origin and destination points in the network [20]. A key unique feature of this work is the consideration of charging coordination, which enables a differentiated analysis of the effects on charging processes and the grid load. In addition, the savings potential of the fast-charging infrastructure is analysed using current data and figures from Austria. The bottom-up model based on this enables a more precise assessment of the savings potential of the fast-charging infrastructure on Austrian highways. Another important contribution of this work is the analysis of the savings potential taking into account seasonal fluctuations and weekend traffic. By examining these factors, changes in network utilisation and energy demand can be better understood, allowing strategies for optimizing the charging infrastructure to be adapted to different traffic and weather conditions.

The specific changes compared to the work of Golab et al. [20] are:

- Changed objective function to maximize fast-charging investment savings
- Calculation of unused charging capacity for each Charging Station (CS)
- Classification of vehicles into two vehicle categories with
  - Different minimum charging quantities, whereby those for vehicles of the charging coordination are not limited
  - Unequal minimum charging times with more flexibility for charging coordination vehicles
  - Various charging windows to start the charging process with a larger window for charging coordination vehicles
- Different fast-charging infrastructure, traffic data, and vehicle parameters
- Sensitivity analyses on the number of vehicles, seasonal and weekend travel pattern

3 Methodology and Data

This chapter provides a detailed explanation of the method used and the mathematical modeling of the optimization model. Further, the input data are described and examined as part of a case study. The software used, its availability, and its complexity are also described.

3.1 Base of Work

This paper is based on the work of Golab et al. [20]. This work considers the increasing charging demand due to the growing fleet of Battery Electric Vehicle (BEV) and the resulting expansion of fast-charging capacity. The proposed optimization model tests the feasibility of planned highway charging infrastructures concerning unused charging capacities and infrastructural bottlenecks. This optimization model is applied to a planned fast-charging infrastructure along the highway network in eastern Austria and shows that the charging infrastructure is considered sufficient. The charging infrastructure also meets the demand under various extreme traffic loads and temperature conditions. Furthermore, no bottlenecks were identified. On the contrary, locations with overestimated charging capacities are identified.

The fast-charging infrastructure used in the model is designed for the year 2030 [21]. 2030 marks a crucial milestone in the fight against climate change, as many national and international climate targets agreed as part of the Paris Agreement are aimed at this year. By then, global greenhouse gas emissions are to be reduced to limit global warming to 1.5°C above pre-industrial levels [2]. For Austria, this means working towards a reduction of 48 percent in the sectors outside the EU emissions trading scheme by 2030 compared to 2005. In addition, the Austrian federal government has set itself the goal of being climate-neutral by 2040 [22].

The failure or success of these targets will determine whether long-term climate tipping points can be avoided, making 2030 a critical milestone for global climate policy. This 2030 assumption also relates to the number of BEVs in Austrian traffic, the vehicle-specific parameters, and the possible charging capacity of the fast-charging stations in the model by Golab et al. [20].

3.2 Spatio-temporal Optimization Model

This work further develops the linear optimization model presented in the preceding section, Section 3.1. This model extension considers a selected fast-charging infrastructure in Austria and the swarm-like departures and route movements of BEV in a time window of 30 hours. The model is designed as a bottom-up method and thus considers the behavior of each individual vehicle. In the following subsections, the most important constraints of the original work and then the extensions are described in more detail.

In contrast to Golab et al. [20], this study refers to the current charging infrastructure and the currently available traffic data. The year 2030, critical for the Paris Agreement, is only 6 years away, but today's BEVs are not quite at the level of the vehicle parameters considered in Golab et al. [20].

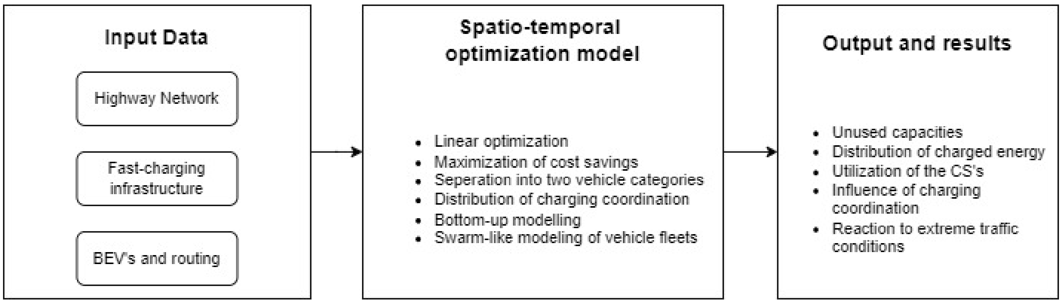

Figure 3.1: Overview of the input files, the optimization model and the most important outputs

3.2.1 Nomenclature

Indices

$r \in R$	*Routes*
$t \in T$	*Time step*
$f \in F_{ALL}$	*All vehicle fleet*
$f \in F_{RND}$	*Random vehicle fleet*
$f \in F_{CTR}$	*Controlled vehicle fleet*
$s \in S_{ALL}$	*All highway Sections*
$s \in S_{CS}$	*Highway segments with ChargingStation*

Table 3.1: Indices of the optimization model

Decision Variables

Cap_s^{unused}	Unused capacity of segment s
t_f^{depart}	Time step t of departure for fleet f
$n_{f,s}^{incoming\_vehicles,t}$	Number of vehicles of fleet f which newly enter a highway segment s at time step t
$Q_{f,s}^{incoming\_vehicles,t}$	Stored energy (kWh) in batteries of vehicles of fleet f newly entering a highway segment s at time step t
$n_{f,s}^{in,t}$	Number of incoming vehicles of fleet f coming into a highway segment s at time step t
$Q_{f,s}^{in,t}$	Stored energy (kWh) in batteries of vehicles of fleet f coming into a highway segment s at time step t
$n_{f,s}^{in\_wait\_charge,t}$	Number of vehicles of fleet f which use the CS in a highway segment s at time step t
$Q_{f,s}^{in\_wait\_charge,t}$	Stored energy (kWh) in batteries of vehicles of fleet f using the CS in a highway segment s at time step t
$n_{f,s}^{in\_charge,t}$	Number of vehicles of fleet f moving to the CS in a highway segment s at time step t
$Q_{f,s}^{in\_charge,t}$	Stored energy (kWh) in batteries of vehicles of fleet f moving to the CS in a highway segment s at time step t
$n_{f,s}^{pass,t}$	Number of vehicles of fleet f which pass the CS in a highway segment s at time step t
$Q_{f,s}^{pass,t}$	Stored energy (kWh) in batteries of vehicles of fleet f passing the CS in a highway segment s at time step t
$n_{f,s}^{finished\_charging,t}$	Number of vehicles of fleet f which finished charging at the CS in a highway segment s at time step t
$Q_{f,s}^{finished\_charging,t}$	Stored energy (kWh) in batteries of vehicles of fleet f which finished charging at the CS in a highway segment s at time step t
$n_{f,s}^{exit,t}$	Total number of vehicles of fleet f which leave a highway segment s at time step t
$Q_{f,s}^{exit,t}$	Stored energy (kWh) in batteries of vehicles of fleet f leaving a highway segment s at time step t
$n_{f,s}^{charge1/2/3,t}$	Number of vehicles of fleet f charging in the CS at highway segment s at first/second/third charging time step t
$n_{f,s}^{arrived\_vehicles,t}$	Number of vehicles of fleet f which arrive at the end of the route in highway segment s at time step t
$Q_{f,s}^{arrived\_vehicles,t}$	Stored energy (kWh) in batteries of vehicles of fleet f arriving the end of the route in highway segment s at time step t

Decision Variables

$n_{f,s}^{out,t}$	Number of vehicles of fleet f which leave a highway segment s at time step t
$Q_{f,s}^{out,t}$	Stored energy (kWh) in batteries of vehicles of fleet f leaving a highway segment s at time step t
$E_{f,s}^{charge1/2/3,t}$	Charged Energy (kW) in segment s for fleet f at first/second/third charging time step t
$E_{f,s}^{consumed\_pass,t}$	Consumed Energy (kW) for fleet f by passing the CS in segment s at time step t
$E_{f,s}^{consumed\_charge\_wait,t}$	Consumed Energy (kW) for fleet f before entering the CS in segment s at time step t
$E_{f,s}^{consumed\_exit\_charge,t}$	Consumed Energy (kW) for fleet f after charging at the CS in segment s at time step t
$n_{f,s}^{queue,t}$	Total number of vehicles of fleet f waiting before charging at highway segment s at time step t
$Q_{f,s}^{queue,t}$	Total stored energy (kWh) in batteries of vehicles of fleet f waiting before charging at highway segment s at time step t
$n_{f,s}^{wait,t}$	Number of vehicles of fleet f waiting before charging at highway segment s at time step t
$Q_{f,s}^{wait,t}$	Stored energy (kWh) in batteries of vehicles of fleet f waiting before charging at highway segment s at time step t
$n_{f,s}^{in\_wait,t}$	Number of vehicles of fleet f newly entering the waiting at highway segment s at time step t
$Q_{f,s}^{wait,t}$	Stored energy (kWh) in batteries of vehicles of fleet f newly entering the waiting line at highway segment s at time step t
$n_{f,s}^{wait\_charge\_next,t}$	Number of vehicles of fleet f waiting but charging next time step at highway segment s at time step t
$Q_{f,s}^{wait\_charge\_next,t}$	Stored energy (kWh) in batteries of vehicles of fleet f waiting but charging next time step a highway segment s at time step t

Table 3.2: Most important decision variables of the optimization model

Parameters

v	$Driving\ speed$	$110\ km/h$
$l^{segment}$	$Length\ of\ each\ segment$	$27.5\ km$
ϵ^{BEV}	$BEV\ share$	$3.5\ \%$
$\epsilon^{long\_distance}$	$BEV\ long\ distance\ share$	$33.\overline{3}\ \%$
$CAP_f^{battery}$	$BEV\ battery\ capacity$	$70\ kWh$
$Cap_s^{segment}$	$Segment\ capacity$	$300 - 2880\ kW$
p^{charge}	$BEV\ charging\ power$	$100\ kW$
η^{charge}	$Charging\ efficiency$	$71.428\ \%$
$d^{consumption}$	$BEV\ energy\ consumption$	$0.20\ kWh/km$
SOC^{init}	$SOC\ during\ initial\ departure\ for\ all\ vehicles$	$60\ \%$
$SOC^{lower\_threshold\_RND}$	$Minimum\ decision\ SOC\ for\ RND\ vehicles$	$20\ \%$
$SOC^{upper\_threshold\_RND}$	$Maximum\ decision\ SOC\ for\ RND\ vehicles$	$40\ \%$
$SOC^{lower\_threshold\_CTR}$	$Minimum\ decision\ SOC\ for\ CTR\ vehicles$	$10\ \%$
$SOC^{upper\_threshold\_CTR}$	$Maximum\ decision\ SOC\ for\ CTR\ vehicles$	$50\ \%$
$SOC^{min\_charging\_RND}$	$Minimum\ SOC\ RND\ vehicles\ charge\ up\ to$	$80\ \%$
t^{min_RND}	$Minimum\ charging\ time\ for\ RND\ vehicles$	$15\ min$
t^{min_CTR}	$Minimum\ charging\ time\ for\ CTR\ vehicles$	$6\ min$
$t^{resolution}$	$Model\ time\ resolution$	$15\ min$
c^{per_kW}	$Expansion\ costs\ per\ kW$	$200\ \frac{EUR}{kW}$

Table 3.3: Optimization model parameters

3.2.2 Objective function

As mentioned in Section 1.2, this work aims to identify possible cost savings for expanding the fast-charging infrastructure, especially for Austria. To achieve this, the model's objective function defines the maximization of these cost savings. The cost savings are calculated from the unused capacities of all cell segments s and the expansion costs per kW. The expansion costs $c^{per\_kW} = 200\frac{EUR}{kW}$ result from a simplified extrapolation for a DC fast-charging station. A DC fast-charging station with a capacity of 150 kW can be estimated at around EUR 30,000. These costs do not include electrical work, installation, grid connection, necessary transformer stations, or civil engineering work. These costs can vary depending on the location and lead to different expansion costs per kW. The averaged factor c^{per_kW} is used as the core indicator for extrapolating the potential cost savings [23].

This results in the following objective function:

$$\max CAP_s^{unused} \cdot c^{per\_kW} \tag{3.1}$$

It should be noted that the objective function used here differs from that of Golab et al. [20] and has therefore been adapted.

3.2.3 Vehicle traffic flow

The linear optimization model is structured to assign each vehicle to a fleet f. Each fleet follows a predefined route r along the implemented highway network. Each fleet movement and each charging process is observed in time step t, and a model time resolution $t^{resolution}$ is defined. Together with the specified driving speed v, this results in a cell segment length $l^{segment}$ of:

$$l^{segment} = v \cdot t^{resolution} \tag{3.2}$$

The structure of a cell segment s with an CS and the associated vehicle movement and charging variables is shown in Figure 3.2. Whether the segment contains an CS depends on the input data based on the actual highway infrastructure.

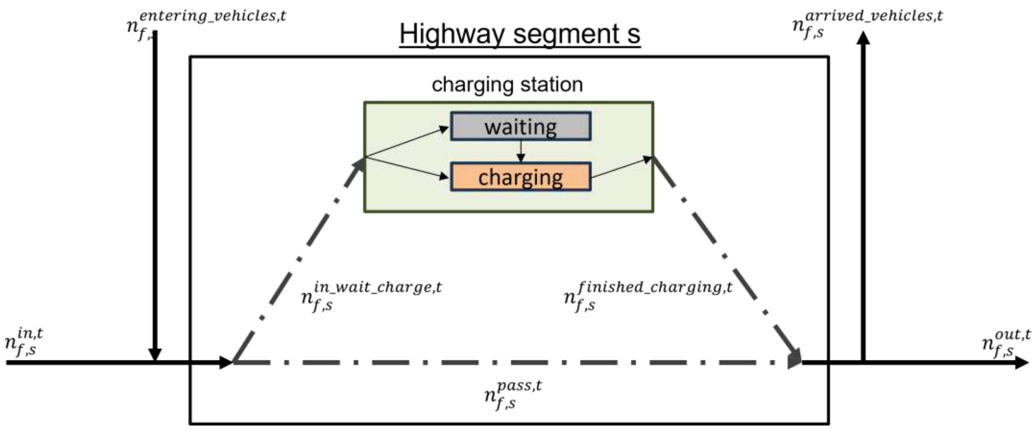

Figure 3.2: Overview of the movement and charging variables of a highway segment with charging station

There are two ways for vehicles to enter a segment s:

- $n_{f,s}^{incoming\_vehicles,t}$ describes vehicles of a fleet f that enter the first segment s of their route r at the departure time of the fleet t^{depart}.

- $n_{f,s}^{in,t}$ describes vehicles of a fleet f that enter another segment s of the route r that is not the first segment of the route at time step t.

In addition, there are two ways to leave a segment s. The total number of vehicles that leave a segment is recorded in the variable $n_{f,s}^{exit,t}$:

- $n_{f,s}^{arrived\_vehicles,t}$ describes vehicles of a fleet f that leave the last segment s of their route r at time step t and therefore do not enter a new segment s.
- $n_{f,s}^{out,t}$ describes vehicles of a fleet f that leave another segment s of their route r that is not the last segment of the route t at time step t and enter a new segment s in the following time step $t+1$.

The variables are linked as follows

$$n_{f,s}^{exit,t} = n_{f,s}^{arrived\_vehicles,t} + n_{f,s}^{out,t} \tag{3.3}$$

To ensure that the vehicles follow the specified route r, the transition from one cell segment s to the next cell segment $s+1$ of the route r is recorded in the routing condition:

$$n_{f,s}^{out,t} = n_{f,s+1}^{in,t} \tag{3.4}$$
$$for\ s\ \epsilon\ r\ without\ last\ route\ segment$$

Each vehicle number variable n is assigned a Q variable, which describes the energy as a function of the number of vehicles for this fleet f in the segment s at time step t and the battery and its State of Charge (SOC). The relationship between n and Q is the same for all variables and is shown for $n_{f,s}^{exit,t}$ in Equation 3.5. Therefore, the available energy $Q_{f,s}^{exit,t}$ lies between a defined minimum and maximum SOC.

$$n_{f,s}^{exit,t} \cdot CAP_f^{battery} \cdot SOC_{min} \leq Q_{f,s}^{exit,t} \geq n_{f,s}^{exit,t} \cdot CAP_f^{battery} \cdot SOC_{max} \tag{3.5}$$

3.2.4 Identification of unused capacities

As the title of this work indicates and as the research questions (Section 1.2) also express, the capacity of the CS in the cell segments plays a crucial role. More precisely, the unused capacity of the cell segments. The unused capacity of a cell is the capacity that is not used at maximum utilization. In the model, the unused capacity is calculated as follows:

$$CAP_s^{unused} = \sum_{s=1}^{S} \left[CAP_s^{segment} - \sum_{f=0}^{F} \left(\frac{E_{f,s}^{charge1,t} + E_{f,s}^{charge2,t} + E_{f,s}^{charge3,t}}{t^{resolution} \cdot \eta^{charge}} \right) \right] \tag{3.6}$$

The Equation 3.6 considers all cell segments S_{ALL} and all fleets F_{ALL} over the entire optimization period without temporal influence. The variable Cap_s^{unused} reflects the unused capacity for each cell segment s. These capacities are calculated from the initial cell segment capacity $CAP_s^{segment}$ minus the charged energy at each of the three charging time points $E_{f,s}^{charge1,t}$, $E_{f,s}^{charge2,t}$ and $E_{f,s}^{charge3,t}$ divided by the time resolution $t^{resolution}$ and the charging efficiency η^{charge}.

The charged energy at a certain charging time step is defined as follows:

$$E_{f,s}^{charge1/2/3,t} \geq n_{f,s}^{charge1/2/3,t} \cdot P^{charge} \cdot \eta^{charge} \cdot t^{resolution} \tag{3.7}$$

P^{charge} [kW] defines the maximum charging power.

3.2.5 Description of the charging process

If vehicles want to perform a charging process, this is only possible in the cell segments containing a CS (S_{CS}). All vehicles that enter a segment s without a CS pass through ($n_{f,s}^{pass,t}$) this segment within one time step and consequently leave this segment in the following time step ($n_{f,s}^{exit,t+1}$). If the cell segment contains an CS, there is the possibility of a charging process for the vehicles ($n_{f,s}^{in\_wait\_charge,t}$).

$$\begin{aligned} & if\ CAP_c^{segment} > 0: \\ & n_{f,s}^{in,t} + n_{f,s}^{incoming\_vehicles,t} = n_{f,s}^{pass,t} + n_{f,s}^{in\_wait\_charge,t} \end{aligned} \tag{3.8}$$

$$\begin{aligned} & else: \\ & n_{f,s}^{in,t} + n_{f,s}^{incoming\_vehicles,t} = n_{f,s}^{pass,t} \end{aligned} \tag{3.9}$$

In the next step, the vehicles entering the CS are divided as follows: Vehicles that start a charging process directly ($n_{f,s}^{in\_charge,t}$) and vehicles that first wait in a queue until a charging process can be attempted ($n_{f,s}^{in\_wait,t}$).

$$n_{f,s}^{in\_wait\_charge,t} = n_{f,s}^{in\_charge,t} + n_{f,s}^{in\_wait,t} \tag{3.10}$$

A queue at time step t is defined as follows:

$$n_{f,s}^{wait,t} = n_{f,s}^{wait,t-1} + n_{f,s}^{in\_wait,t} - n_{f,s}^{wait\_charge\_next,t} \tag{3.11}$$

Vehicles that can start charging immediately at time step t:

$$n_{f,s}^{charge1,t} = n_{f,s}^{in\_charge,t} + n_{f,s}^{wait\_charge\_next,t-1} \tag{3.12}$$

The charging process can last up to 3 time steps. Here, $n_{f,s}^{charge1,t}$ is the variable that represents all vehicles in a fleet f in the segment s that have just started the charging process. After a time step, it is possible to end the charging process ($n_{f,s}^{finished\_charge1,t}$) or to charge a further time step ($n_{f,s}^{charge2,t}$). This process can also be repeated for a third charging time step. After the third time step, the charging process is terminated in any case. The relationships are as follows:

$$n_{f,s}^{output\_charged1,t} = n_{f,s}^{charge1,t-1} = n_{f,s}^{finished\_charge1,t} + n_{f,s}^{charge2,t} \tag{3.13}$$

$$n_{f,s}^{output\_charged2,t} = n_{f,s}^{charge2,t-1} = n_{f,s}^{finished\_charge2,t} + n_{f,s}^{charge3,t} \tag{3.14}$$

$$n_{f,s}^{output\_charged3,t} = n_{f,s}^{charge3,t-1} = n_{f,s}^{finished\_charge3,t} \tag{3.15}$$

All vehicles that end a charging process in the same time step t are grouped:

$$n_{f,s}^{finished\_charging,t} = n_{f,s}^{finished\_charge1,t} + n_{f,s}^{finished\_charge2,t} + n_{f,s}^{finished\_charge3,t} \tag{3.16}$$

Analog to Equation 3.8 and Equation 3.9 for vehicles leaving a segment s:

$$
\begin{aligned}
&if\ CAP_c^{segment} > 0: \\
&n_{f,s}^{exit,t+1} = n_{f,s}^{finished\_charging,t} + n_{f,s}^{pass,t}
\end{aligned} \tag{3.17}
$$

$$
\begin{aligned}
&else: \\
&n_{f,s}^{exit,t+1} = n_{f,s}^{pass,t}
\end{aligned} \tag{3.18}
$$

When passing, entering, and leaving a CS, energy is consumed from the vehicle batteries ($CAP_f^{battery}$). This model assumes that the CS is always located exactly in the middle of a segment. The consumed energies are calculated as follows:

$$E_{f,s}^{consumed\_pass,t} = n_{f,s}^{pass,t} \cdot l^{segment} \cdot d^{consumption} \tag{3.19}$$

$$E_{f,s}^{consumed\_charge\_wait,t} = n_{f,s}^{in\_wait\_charge,t} \cdot \frac{1}{2} \cdot l^{segment} \cdot d^{consumption} \tag{3.20}$$

$$E_{f,s}^{consumed\_exit\_charge,t} = n_{f,s}^{finished\_charging,t} \cdot \frac{1}{2} \cdot l^{segment} \cdot d^{consumption} \tag{3.21}$$

3.2.6 Definition of vehicle categories

In this model, a differentiation is made between two vehicle categories.

- Random (RND): The first category includes vehicles expected to behave like actual users of BEV on the highway.
- Controlled (CTR): The second category includes vehicles that are part of a charging coordination and thus receive spatial and temporal specifications for the charging process.

Constraints in charging behavior can be identified for both vehicle categories, which can be divided into three categories:

- SOC window: This refers to the vehicle SOC when a charging process should start
- Time: The minimum amount of time a charging process takes
- Amount of energy: The minimum energy charged into the vehicle battery

Vehicles in the RND category can start charging as soon as the SOC falls below 40 percent ($SOC^{upper\_threshold\_RND}$). The lower limit and, therefore, the latest possible charging time is set at 20 percent SOC ($SOC^{lower\_threshold\_RND}$) due to range anxiety. Range anxiety, a phenomenon that occurs particularly with BEVs, describes the concern of users regarding a possible shortfall in range and the availability of charging infrastructure. This feeling often leads to drivers of BEVs taking charging breaks earlier than necessary in order to prevent potential bottlenecks - a behavior that is generally less pronounced in vehicles with combustion engines due to the extensive network of filling stations [7]. Since charging an BEV takes longer than refueling a conventional vehicle and the charging process is often combined with a break, the minimum charging time for RND vehicles is 15 minutes (t^{min_RND}). In addition, vehicles in the RND category are charged to at least 80 percent SOC before leaving the CS.

The second vehicle category (CTR) reflects the idea of charging coordination, which aims to enable a better response to the current situation by providing charging instructions. On the one hand, this aims to avoid queues and, on the other, to use the available capacity more efficiently and thus generate capacity savings. Therefore, the controllable vehicles' charging processes can be adapted in terms of space and time to the current situation and provide the participants in this charging coordination with a spatial and temporal charging specification based on their route. In order to make this possible, vehicles in the CTR category have greater flexibility in starting the charging process and varying the duration and charging quantity. A charging process can already be started at a SOC of 50 percent ($SOC^{upper\_threshold\_CTR}$), with the lower limit being 10 percent SOC ($SOC^{lower\_threshold\_CTR}$). A charging process can be ended after just 6 minutes (t^{min_CTR}). Beyond this, there are no further restrictions regarding the minimum energy charged. This characteristic enables vehicles in the CTR category to react to the behavior of vehicles in the RND category.

The constraints implemented in the model for the charging window of the two vehicle categories are defined as follows:

$$Q_{f,s}^{in\_charge,t} \leq n_{f,s}^{in\_charge\_wait,t} \cdot CAP_f^{battery} \cdot SOC^{upper\_threshold\_RND} \tag{3.22}$$

$$Q_{f,s}^{in\_charge,t} \geq n_{f,s}^{in\_charge\_wait,t} \cdot CAP_f^{battery} \cdot SOC^{lower\_threshold\_RND} \tag{3.23}$$

$$for\ s \epsilon S_{CS},\ f \epsilon F_{RND}\ and\ t \epsilon T$$

$$Q_{f,s}^{in\_charge,t} \leq n_{f,s}^{in\_charge\_wait,t} \cdot CAP_f^{battery} \cdot SOC^{upper\_threshold\_CTR} \tag{3.24}$$
$$Q_{f,s}^{in\_charge,t} \geq n_{f,s}^{in\_charge\_wait,t} \cdot CAP_f^{battery} \cdot SOC^{lower\_threshold\_CTR} \tag{3.25}$$

$$for\ s \epsilon S_{CS},\ f \epsilon F_{CTR}\ and\ t \epsilon T$$

The cumulative energy ($Q_{f,s}^{in\_charge,t}$) of the vehicles of a fleet f moving to the CS in segment s at time step t is compared with the upper and lower SOC limits of the respective charging window. The charging windows illustrated can be found in Figure 3.3. The vehicles in the CTR category are shown in blue in the figure, while the vehicles in the RND category are shown in orange.

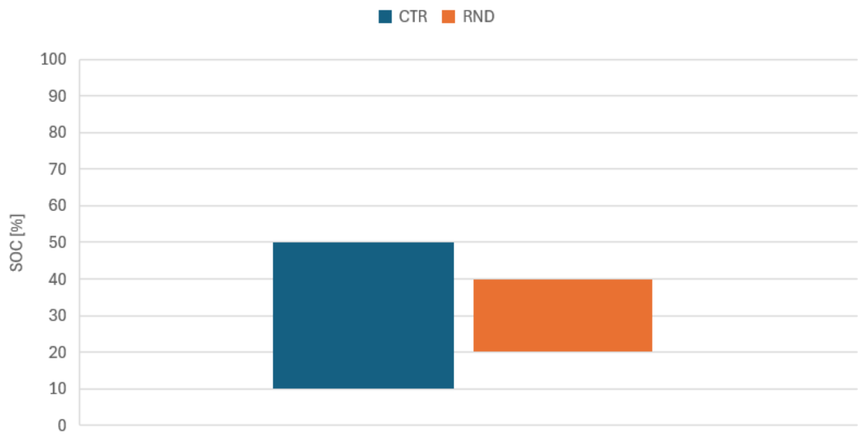

Figure 3.3: Charging windows for CTR (blue) and RND (orange) vehicles

The defined minimum charging times imply specific constraints for the charged energy of the three charging time steps:

$$E_{f,s}^{charge_1,t} \geq n_{f,s}^{in\_charge,t} \cdot P^{charge} \cdot \eta^{charge} \cdot t^{min\_RND} \tag{3.26}$$
$$E_{f,s}^{charge2,t} \geq n_{f,s}^{in\_charge,t} \cdot P^{charge} \cdot \eta^{charge} \cdot t^{min\_RND} \tag{3.27}$$
$$E_{f,s}^{charge_3,t} \geq n_{f,s}^{in\_charge,t} \cdot P^{charge} \cdot \eta^{charge} \cdot t^{min\_RND} \tag{3.28}$$
$$for\ s \epsilon S_{CS},\ f \epsilon F_{RND}\ and\ t \epsilon T$$

$$E_{f,s}^{charge1,t} \geq n_{f,s}^{in\_charge,t} \cdot P^{charge} \cdot \eta^{charge} \cdot t^{min\_CTR} \tag{3.29}$$

$$E_{f,s}^{charge2,t} \geq n_{f,s}^{in\_charge,t} \cdot P^{charge} \cdot \eta^{charge} \cdot t^{min\_CTR} \tag{3.30}$$

$$E_{f,s}^{charge3,t} \geq n_{f,s}^{in\_charge,t} \cdot P^{charge} \cdot \eta^{charge} \cdot t^{min\_CTR} \tag{3.31}$$

$$for\ s \epsilon S_{CS},\ f \epsilon F_{CTR}\ and\ t \epsilon T$$

The minimum charging times for the two vehicle categories and the time resolution ($t^{resolution}$) are shown in Figure 3.4.

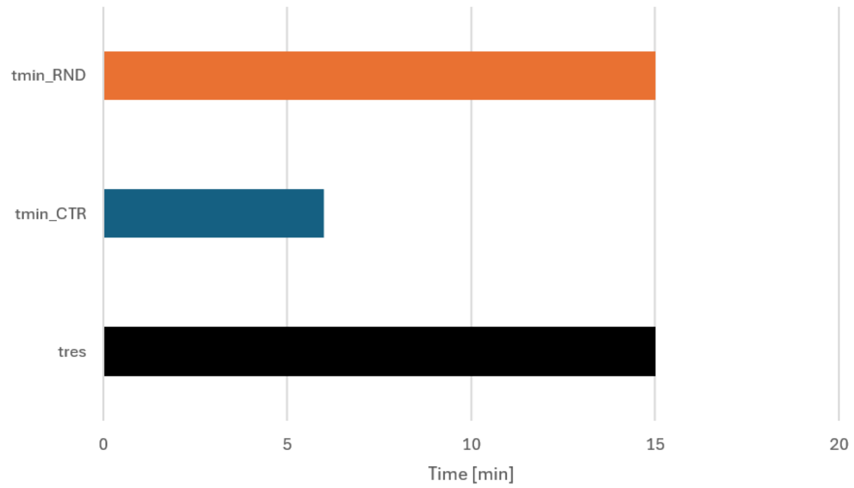

Figure 3.4: Minimum charging times for CTR (blue) and RND (orange) vehicles and the time resolution of the model

Based on the restriction that vehicles in the RND category must charge to at least 80 percent SOC, the following condition results for the cumulative energy ($Q_{f,s}^{finished\_charging,t}$) of the vehicles of the fleet f that have completed the charging process in segment s at time step t:

$$Q_{f,s}^{finished\_charging,t} \geq n_{f,s}^{finished\_charging,t} \cdot CAP^{battery} \cdot SOC^{min\_charging\_RND} \tag{3.32}$$

$$for\ s \epsilon S_{CS},\ f \epsilon F_{RND}\ and\ t \epsilon T$$

The mandatory charging quantity for the two vehicle categories is shown in Figure 3.5.

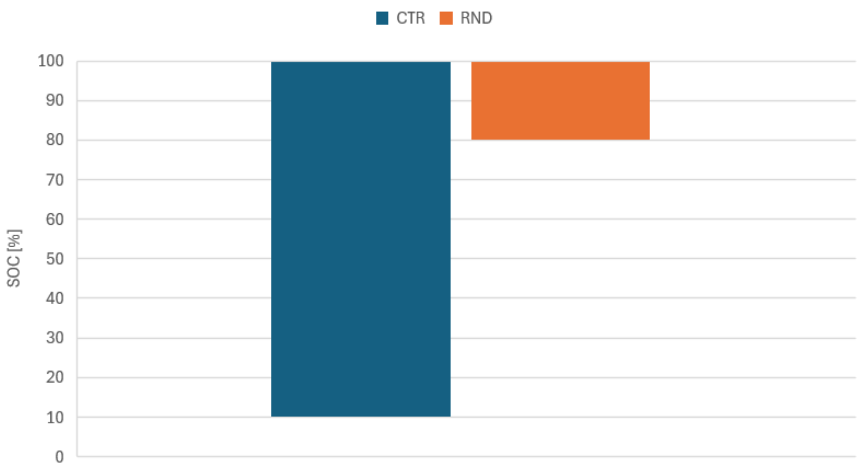

Figure 3.5: charging quantity for CTR (blue) and RND (orange) vehicles

Both vehicle categories are added to the optimization model. The specifications for vehicles in the RND category are defined much more strictly and in greater detail than those in the CTR category. The solver, therefore, optimizes all vehicles in the model. However, the stricter specifications for RND vehicles influence the results and the behavior of CTR vehicles, particularly on the influence of charging coordination and the possible capacity savings.

3.2.7 Maintaining the traffic flow

This work aims to identify unused capacities (Subsection 3.2.4) without blocking the traffic flow. For this purpose, it is necessary to define restrictions for the queue, the definition of which can be seen in Equation 3.11.

The queue consists of the vehicles that have already waited in the last time step ($n_{f,s}^{wait,t-1}$), the vehicles that are new to the queue ($n_{f,s}^{in\_wait,t}$) and the vehicles that will start charging in the next time step ($n_{f,s}^{wait\_charge\_next,t}$).

To eliminate the risk of queuing, two essential constraints are strategically integrated into the model:

$$n_{f,s}^{wait\_charge\_next,t} = 0 \tag{3.33}$$

$$n_{f,s}^{wait,t} = 0 \tag{3.34}$$

$$for\ s\ \epsilon\ S_{CS},\ t\ \epsilon\ T\ and\ f\ \epsilon\ F_{ALL}$$

The implementation of Equation 3.33 and Equation 3.34 ensures that there are no queues at the CS, that every vehicle can be charged immediately, and therefore that traffic flow is not impeded.

3.2.8 Model availability and complexity

This master thesis develops an optimization model in *Python* [24] based on the *Anaconda* distribution [25] and the integrated development environment *PyCharm* [26]. *Pyomo* is used to model the optimization problem, which enables a flexible formulation of linear and non-linear problems that are solved with external solvers [27]. For data processing and analysis, *pandas* and *numpy* are used: *pandas* for efficient data manipulation [28] and *numpy* for fast numerical calculations [29]. This combination of software provides a powerful environment for the development and implementation of the model. As usual in optimizations, float numbers are used in this model, and integer variables for the number of vehicles were deliberately avoided to avoid unnecessarily increasing the computing time per optimization. Modeling without integers reduces complexity and enables a more efficient solution to the problem so that the model can react more quickly to optimizations. This configuration allows the model to be solved quickly and accurately, even with complex and large data. The model contains more than 920,000 constraints and over 560,000 variables. Float numbers reduce the required computing time per optimization to less than 3 minutes.

This thesis uses the *Gurobi* solver to solve the optimization model [30]. *Gurobi* is a powerful commercial solver specially developed for mathematical optimization problems such as linear and mixed-integer programming. The parameter "Method = 2" is used in the implementation, whereby the barrier algorithm is used to solve the model. This algorithm is particularly suitable for large and dense linear programs, offering greater computing efficiency. In addition, the crossover step is deactivated, which further reduces the calculation time, as this step is not required for many applications and can speed up the solving of the model.

3.3 Data Input and Case Study

Two different input data are relevant for testing the described model.

- Cell segment input: In this file, the highway environment is defined with its segments s and possible Charging Station (CS).
- Fleet input: The vehicle fleets f and their assigned routes r, vehicle parameters, and departure times are defined in this file.

The cell segment input file represents the fast-charging infrastructure and the fleet input file represents the charging capacity demand of BEVs for this infrastructure.

3.3.1 Segment Input

Part of the required input data for the optimization is the geography of the highway road network used. The imported segment file contains information describing the individual cell segments s. In addition to the identification number of the cell segment, the file contains the length of the segment in km. The file also contains information about fast-charging stations along the highway. The identifier *has_cas* indicates whether a CS is available. The *Capacity* information indicates the charging capacity available in this cell segment in kW. The informations defined in the cell segment input file can be seen in Table 3.4.

Item	Description
cell_id	Identifier for this specific segment
length	Length of the segment
capacity	Amount of charging capacity this segment
has_cs	Identifier if the segment has a charging station

Table 3.4: Cell segment input data description

3.3.2 Fleet Input

The second part of the input files describes the vehicle fleets f and their routes r along the highway network. The fleets f are formed by grouping all vehicles traveling the same route r. The number of these vehicles is stored in $fleet\_size$, but the departure times within a fleet can vary and are defined in *depart_time*. The time step of the first departure of a vehicle within this fleet is represented by *start_timestep*. The departure times of the vehicles can be distributed over the entire time resolution of the model ($t^{resolution}$) and will be discussed in more detail later. Each fleet is assigned a fixed value for the battery capacity per vehicle, the charging power, the specific consumption per kilometer driven, and the battery SOC value for entering the highway network, as well as information about the number of cell segments of the fleet route r. Further a identifier supplies the fleets f with a number. The last parameter of the fleet file is information about the fleet vehicle category. Two different categories are available for categorizing the vehicles, which are explained in detail in Subsection 3.2.6. The parameter *vehicle_category* takes the value 1 or 0 for the respective vehicle category.

The parameters defined in the fleet input file are listed in the table below.

Item	Description
start_timestep	Time step of the first departure
route	Chain of the used segments in order
fleet_size	Amout of cars
charge_cap	Indicates the charging speed [kW]
batt_cap	Indicates the total battery capacity [kWh]
d_spec	Indicates the specific consumption of the vehicle [kWh/km]
SOC_init	Indicates the SOC at the entrance
incoming	Indicates how many vehicles depart in which segment
arriving	Indicates how many vehicles arrive in which segment
depart_time	Indicates at which time step how many vehicles depart
len	Specifies the number of contiguous segments in the route
fleet_id	Identifier for this specific fleet
vehicle_category	Indicates the vehicle category

Table 3.5: Fleet input data discription

3.3.3 Case Study

The optimization model is evaluated and validated using a case study based on the Austrian A2 highway. Due to its important position in the national traffic network and the associated high traffic load, this highway represents an ideal test platform for a practice-oriented analysis. Actual traffic statistics are used for fleet modeling, which provides insights into vehicle volumes, traffic patterns, and driving dynamics. By combining this data with the specific infrastructure of the A2, the optimization model can be evaluated under realistic conditions.

Austrian Highway A2

A highway from the Austrian highway network is used to evaluate the results, namely the A2 Südautobahn, which extends over a total length of 379.332 km, making it the longest highway in Austria. The A2 connects not only the capital of Austria (Vienna) with the Italian border at Arnoldstein but also the second largest city in Austria and the capital of Styria, Graz, and the capital of Carinthia, Klagenfurt am Wörthersee (hereinafter referred to simply as Klagenfurt). These four places are of particular interest on this highway and therefore Point of Interest (POI). The highway is particularly popular in the summer months, connecting tourists from the Czech Republic, Slovakia, and Poland with the Adriatic Sea [31]. The course of the A2 highway is shown in Figure 3.6.

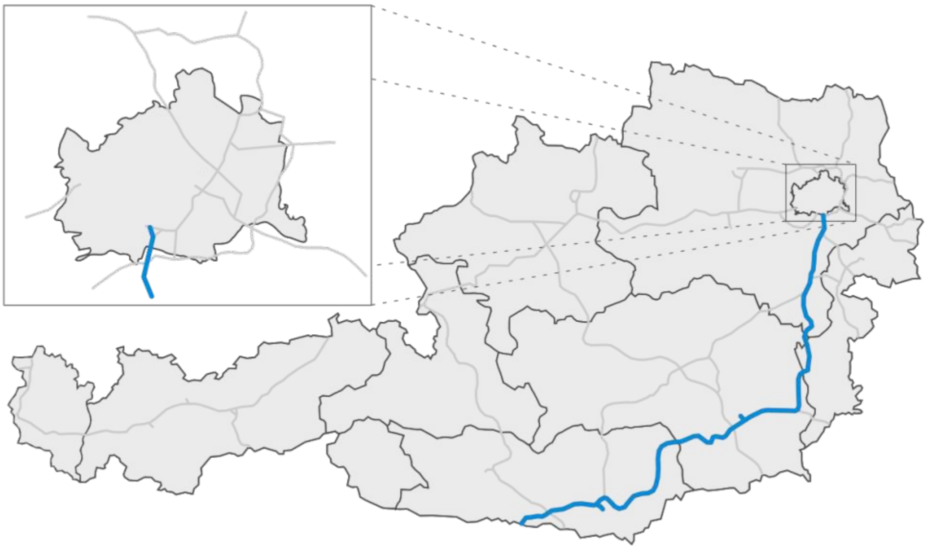

Figure 3.6: Overview of the highway A2 between Vienna and italy (Source: Alexander Wagner, CC BY-SA 3.0 [32])

The segment length is calculated based on the defined vehicle speed v and the time resolution $t^{resolution}$. This connection can be seen in Equation 3.2. For the Austrian highway network, the maximum permitted speed is 130 $\frac{km}{h}$ [33] As it is not possible to drive continuously at maximum speed due to construction sites and temporary speed limits, a reduced speed of the BEVs of $v = 110\ \frac{km}{h}$ is assumed in this model. This results in a segment length of:

$$l^{segment} = 110\ \frac{km}{h} \cdot 0,25\ h = 27.5\ km \tag{3.35}$$

Considering the total length of the A2 highway, 379.332 km, this results in 14 segments.

$$C = 379.332\ km/27.5\ km \approx 14\ segments \tag{3.36}$$

In December 2024, 46 rest areas in Austria have e-charging stations for BEVs [34]. Seven of these 46 rest stops with different capacities are located along the A2, resulting in 10,355 kW total charging power provided by the Autobahnen- und Schnellstraßen-Finanzierungs-Aktiengesellschaft (ASFINAG). An overview of the cells, the position of the POI, the position of the individual rest areas, and information about the available charging capacities are listed in Table 3.6.

Segment-ID	POI	has CS	Name of rest area	Capacity [kW]
01	Vienna	yes	Guntramsdorf	993
02	-	yes	Föhrenberg	2,880
03	-	yes	Zöbern	300
04	-	no	-	-
05	-	no	-	-
06	-	no	-	-
07	Graz	yes	Kaiserwald	2,244
08	-	no	-	-
09	-	no	-	-
10	-	no	-	-
11	-	yes	Völkermarkt	1,451
12	Klagenfurt	no	-	-
13	-	yes	Wörthersee	985
14	Italy	yes	Dreiländereck Nord	1,502

Table 3.6: Overview of the 14 segments of the A2

The exact locations of the rest areas in Table 3.6 can be viewed on the ASFINAG website [34].

Vehicle fleet movement and routing

ASFINAG publishes the results of its monthly traffic count on its website and has also provided annual traffic statistics since 2012 [35]. ASFINAG operates around 270 permanent counting stations in Austria in 2024. Overhead detectors (the combination of ultrasound, passive infrared, and radar is used to draw conclusions about the speed and size of a vehicle) and induction loops (wire loops laid in the roadway generate a weak alternating magnetic field that is changed by vehicles driving over it) are used for evaluation [35]. The locations of the counting stations can be found on the base map [36]. As the data only contains counting stations and the vehicles counted at them, it is impossible to extract vehicle movements for vehicle fleets directly from this data. Therefore, the traffic statistics data (annual statistics 2023) are used in this work as inspiration and reference points to generate fleet movements for the optimization model. The ASFINAG traffic statistics provide vehicle values per 24 hours for different days and day combinations. The current share of Battery Electric Vehicle (BEV) in Austria is $\epsilon^{BEV} = 3.5\ \%$ [5]. Together with the assumption that one-third of all BEVs are eligible for a long-distance consideration ($\epsilon^{longdistance} = 33.\overline{3}\ \%$), the counting point data is downscaled as follows.

First, all counting stations are assigned to the corresponding cell segments. Based on this, the counting station value for an average day (Monday to Sunday) of each cell with the lowest number of vehicles is extracted. This ensures that the used numbers always cover the vehicles that are at least on the entire highway section. The counting points are then assigned to the respective direction of travel. A distinction is made between the direction of Vienna to Italy (S1 to S14) and Italy to Vienna (S14 to S1). In addition, relevant routes are defined and considered in the case study. The points of interest (POI) from the previous chapter serve as a basis. From these four points, 10 interesting routes are extracted. The routes Klagenfurt to Italy and Italy to Klagenfurt are not considered, as they have a cell segment length of 3 segments and are therefore not suitable for a long-distance analysis. The ten routes considered are shown in the following table:

Fleet-ID	Start of route	End of route	Length of route
00	S1 (Vienna)	S14 (Italy)	14
01	S14 (Italy)	S1 (Vienna)	14
02	S1 (Vienna)	S7 (Graz)	7
03	S7 (Graz)	S1 (Vienna)	7
04	S1 (Vienna)	S12 (Klagenfurt)	12
05	S12 (Klagenfurt)	S1 (Vienna)	12
06	S7 (Graz)	S12 (Klagenfurt)	6
07	S12 (Klagenfurt)	S7 (Graz)	6
08	S7 (Graz)	S14 (Italy)	8
09	S14 (Italy)	S7 (Graz)	8

Table 3.7: Overview of the 10 routes

The fleets are assigned according to the direction of travel, with fleets with even identification numbers assigned to the direction from Vienna to Italy and fleets with odd identification numbers assigned to the direction from Italy to Vienna. The smallest number of vehicles in the counting stations per segment is then listed for both travel directions. The two factors ϵ^{BEV} and $\epsilon^{longdistance}$ can then be used to calculate the BEVs relevant for this case study. The smallest value of all segments is the one in segment 14 (Italian border), which specifies the vehicles for the two "Italy routes" of both directions Vienna to Italy/Italy to Vienna and Graz to Italy/Italy to Graz, as these vehicles on these routes are the only ones that actually cross the Italian-Austrian border. These vehicles are now subtracted from the values of the other segments. The following smallest value in cell 8 represents the vehicles for the routes Vienna to Klagenfurt / Klagenfurt to Vienna and Graz to Klagenfurt / Klagenfurt to Graz. The smallest value calculated in segments 1 to 7 represents the vehicles for the remaining routes, Vienna to Graz and Graz to Vienna. Based on these calculated figures, a percentage distribution of the vehicles on the respective route is calculated.

The counting statistics and the calculation result in 154 vehicles on the Vienna to Italy route and 139 vehicles on the Italy to Vienna route, for a total of

$$\sum_{t=0}^{T}\sum_{f=0}^{F}\sum_{s=1}^{S} n_{f,s}^{incoming\_vehicles,t} = 293\ vehicles \tag{3.37}$$

over 24 hours.

The traffic data published by ASFINAG does not allow an exact classification of departures over 24 hours. In the available studies, Datla et al. [37] and Thomas et al. [38] analyze the traffic volume throughout the day. Inspired by these two studies, the various optimizations follow the following scheme, where possible. The scheme is shown in Figure 3.7

In the model shown here, departures are only possible on the hour. Traffic is at its lowest in the late evening, night and early morning hours. The number of departures increases from around 3 a.m., reflecting morning work traffic. Departures peak at 7 a.m., fall slightly over the midday hours and rise again towards the late afternoon. After-work traffic leads to a significant increase in the volume of vehicles on the roads. The optimization is based on a percentage distribution of departures over the hours of the day, resulting in a total of 100 percent over 24 hours. The allocation of the number of vehicles to the various departure times is based on this percentage distribution. The model spans a total of 120 time steps, each lasting 15 minutes. This corresponds to a time horizon of 30 hours. However, the departures of the vehicles are only considered within a 24-hour framework, corresponding to 96 time steps. The remaining six hours represent a buffer to ensure that each vehicle can complete its route in full.

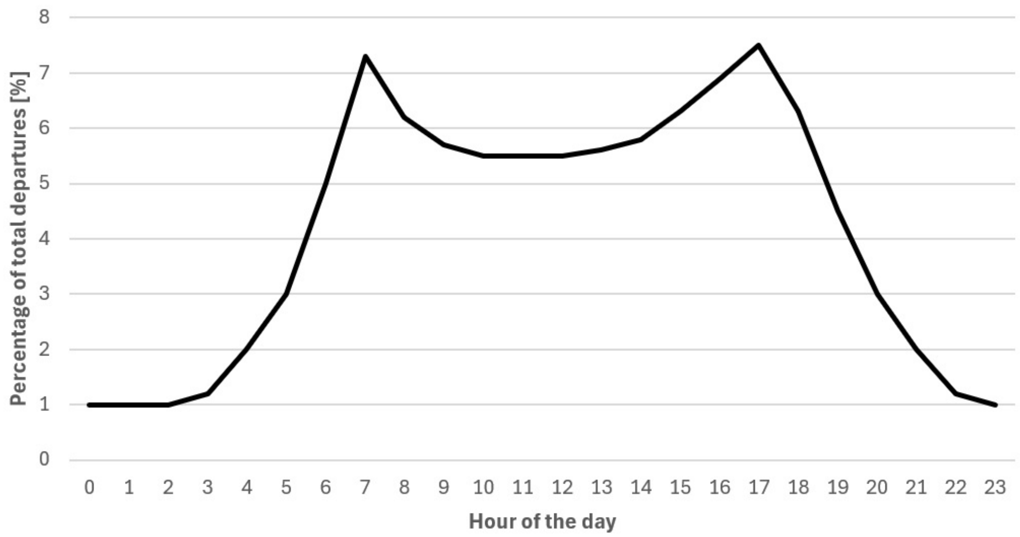

Figure 3.7: Percentage distribution of departures over 24 hours

Finally, the routes are assigned to the two vehicle categories. The exact assignment depends on the percentage distribution of the charging coordination. For this purpose, fleet IDs 10 to 19 are added to the fleet input file. Fleets 00 and 10 are identical, as are fleets 01 and 11, and so forth. Fleets 00 to 09 belong to the CTR category, while fleets 10 to 19 belong to the RND category in this case study. For the consideration of different charging coordination expansion stages , 101 different fleet input data are generated. The percentage distribution of vehicles is adjusted in steps of 1 percent from an initial 100 percent RND vehicles to 100 percent CTR vehicles. As part of the optimization, the 293 BEVs are first categorized into the categories CTR and RND, depending on the percentage charging coordination distribution. Based on this, the vehicles are assigned to the two directions of travel and the different routes for each direction. The departure times are assigned based on the percentage time distribution over 24 hours (92 time steps). The optimizations are carried out according to the procedure described in the Subsection 3.2.2, which aims to maximize the potential investment savings of the fast-charging infrastructure on Austrian highways.

The segment and fleet input data are based on the most up-to-date values available at the time of the work and, therefore, reflect the status quo. The implemented vehicle data is also designed based on the current vehicle data. The classification of BEVs into different categories [39] serves as a guide, with the mid-size class being used as a reference. The *BMW iX3 Impressive*, for example, can be assigned to the mid-size class category. Based on the range and consumption data for this car [40], a battery size of $CAP_f^{battery} = 70\ kWh$ and a consumption of $d^{consumption} = 0.20\ \frac{kWh}{km}$ are defined, which enables a maximum range of 350 km.

$$Maximum\ Range\ of\ BEV = 70\ kWh/0.2\ \frac{kWh}{km} = 350\ km \tag{3.38}$$

The range of BEVs has steadily increased over the years. While the average range in 2010 was 123 km, it is 393 km on average in 2023 [40]. This implies that BEVs could cover the entire length of the A2 highway without recharging. However, most vehicles will generally not enter the highway network with a full battery. Most vehicles have to use country roads and expressways first or start their journey on another highway. In order to adequately implement this behavior in the model, all initial battery SOC (SOC_{init}) are parameterized to 60 percent, which results in a good average for all vehicles. This means that vehicles that have covered a longer distance before reaching the highway, vehicles that have previously driven on other highways, vehicles that first had to use country roads and expressways to join the highway, and vehicles that start their journey on the highway with a full battery are taken into account.

The code, generated fleet input files, and the cell segment input files can be taken from the GIT repository:
`https://github.com/JulesFrdrch/PotentialSavingOnCapacity`

4 Results

This chapter presents the results of the work. First, the model is evaluated using the case study's data. Based on the results and the research questions from Section 1.2, sensitivity analyses focus on capacity savings, the influence of the number of vehicles considered, the seasonal influence, and the influence of the weekend travel pattern.

4.1 Cost savings through charging coordination

Based on the fleet input data, the resulting origin-destination movements with time-distributed departures over 24 hours, and the categorization of the vehicles into two different categories with different behavior, the first step is to take a closer look at the influence of charging coordination with increasing percentage distribution of charging coordination. The following Figure 4.1 illustrates the potential savings in millions of euros as a function of charging coordination in percent.

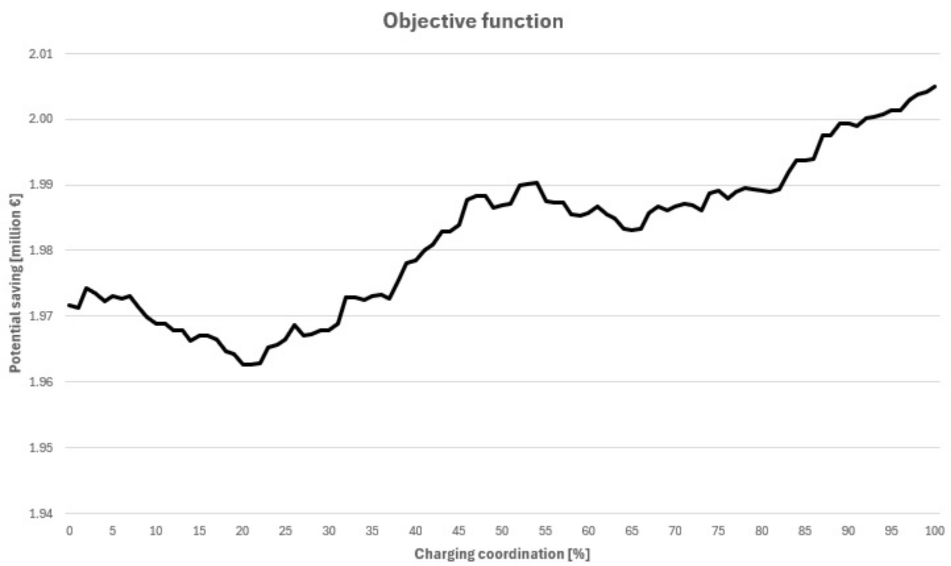

Figure 4.1: Potential savings in millions of euros as a function of charging coordination in percent

The Figure 4.1 shows that a full charging coordination share of 100 percent results in significantly higher potential investment and capacity savings than in the scenario without charging coordination (0 percent). Without charging coordination, cost savings of EUR 1,971,568.65 would be possible. This corresponds to an unused capacity of 9,857.84 kW and a utilization of only 4.8 percent of the available capacity. The introduction of charging coordination makes it possible to reduce the required capacity further and thus optimize cost savings. In a possible scenario in which all 293 vehicles are part of a charging coordination, a maximum investment saving of EUR 2,004,954.36 and thus a capacity saving of 10,024.77 kW would be possible. This means that only 3.189 percent of the expanded capacity would be used. Compared to an optimization without charging coordination, the introduction of full charging coordination enables an increase in cost savings of EUR 33,385.71 along the Austrian A2 highway. This confirms the conclusions of Golab et al. [20] of the over-sizing of the fast charging network in Austria and the fact that the expanded charging capacities would never be fully utilized. The combination of an over-sized fast-charging infrastructure and a low electric-vehicle rate (3.5 percent [5]) in Austria generates significant savings potential that a coordinated charging strategy can further increase.

In addition, an unexpected trend in the objective function can be seen and observed that the objective function decreases between 7 and 20 percent and between 50 and 65 percent charging coordination. The objective function is expected to steadily improve and increase as the proportion of vehicles that comply with charging coordination increases. This effect will be discussed in more detail later and examined more closely with the help of sensitivity analyses (Section 4.2).

First, detailed insights into the results and the associated verification of the model are provided. The scenario with a charging coordination of 25 percent and 75 percent RND vehicles is examined. According to the available data, 73 of the 293 vehicles are assigned to the CTR category, while 220 vehicles are assigned to the RND category.

The Figure 4.2 and Figure 4.3 illustrate two specific battery states of all vehicles in a category, shown over all time steps t and all segments s. The battery states shown are classified as follows

- Blue: The charging process is started
- Orange: The charging process has been completed and the charging station is being exited

It is clear that vehicles in the RND category start the charging process in a range between 20 and 40 percent SOC and leave the charging station with at least 80 percent, while vehicles in the CTR category adhere to the prescribed charging entry window of 10 to 50 percent SOC. The energy charged is not limited, but at least six minutes.

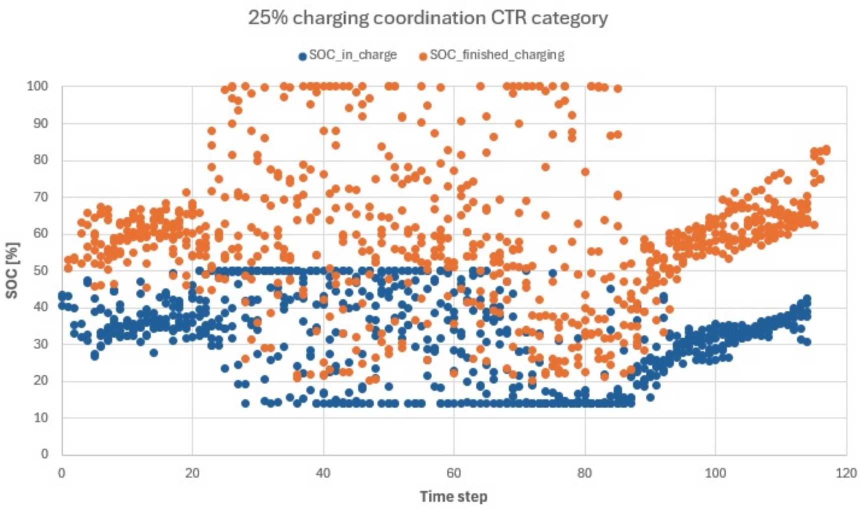

Figure 4.2: SOC of the vehicles in the CTR category during the start of the charging process (blue) and during the end of the charging process (orange) over all time steps

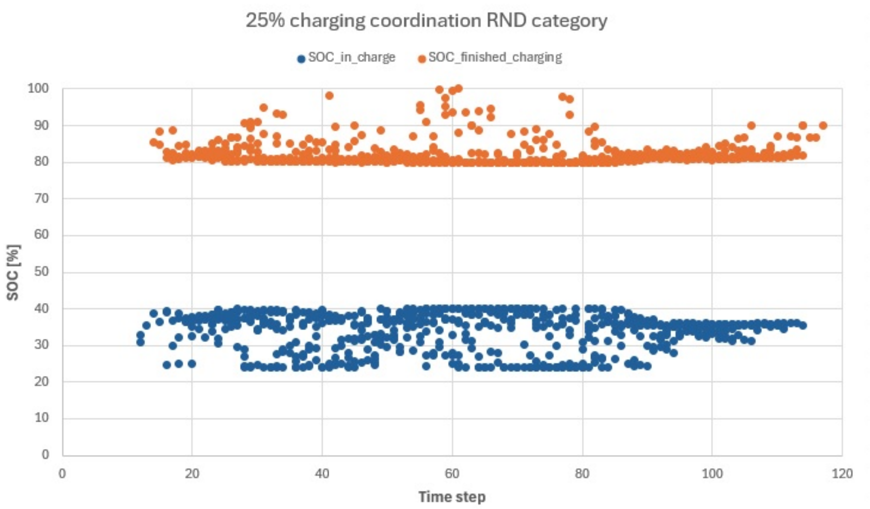

Figure 4.3: SOC of the vehicles in the RND category during the start of the charging process (blue) and during the end of the charging process (orange) over all time step

Thanks to the increased flexibility, CTR vehicles can adapt to the circumstances and distribute the charged energy and the maximum charging capacities used effectively.

The Figure 4.4 illustrates the distribution of total charging energy in MWh as well as the respective shares of RND and CTR vehicles in the various percentage distributions of charging coordination.

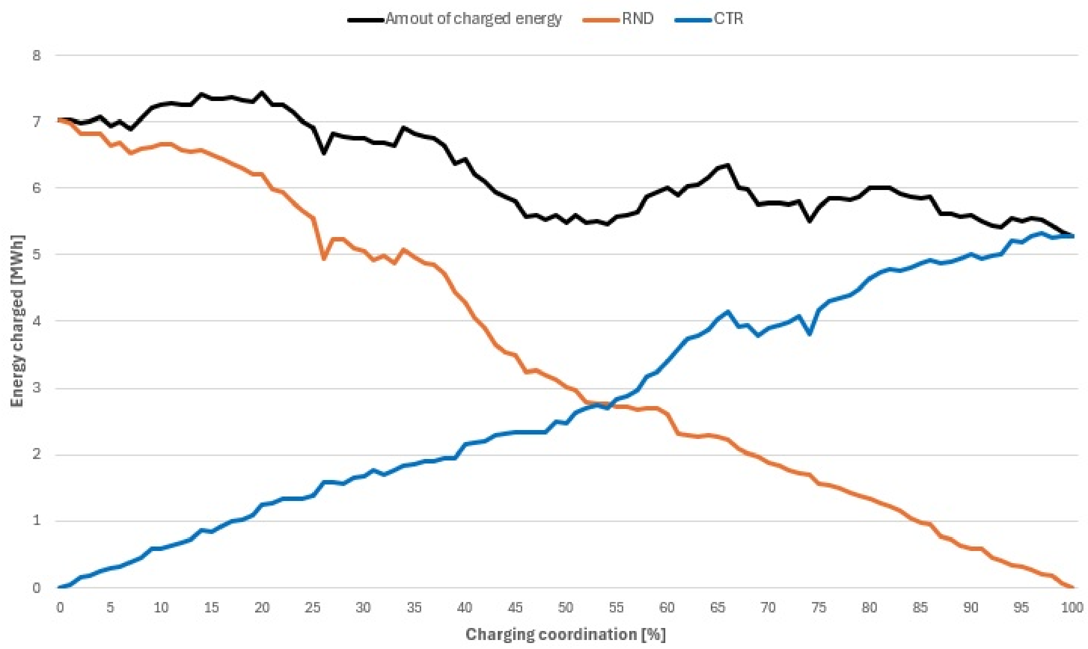

Figure 4.4: Total charged energy [MWh] and the distribution between the two categories over the different percentage distributions of the charging coordination share

4.2 Sensitivity analyses

As already explained, the objective function does not show the expected steady increase as the share of charging coordination increases. A possible explanation for this behavior lies in the number of vehicles surveyed. In the defined case study, the relevant BEV shares are determined based on ASFINAG counting station data. According to this, only 293 BEVs use the A2 highway over 24 hours. This number is very low, as on average, only around 12 BEV use the highway every hour. This low number could be responsible for the course of the objective function. As part of the case study, the vehicle numbers and route distributions are generated using ASFINAG's 2023 annual statistics, which represent an average value for the entire year. However, it should be noted that BEVs behave differently in different seasons. For example, the consumption of BEVs is significantly higher in winter than in summer [41]. In addition, traffic on highways in different seasons is influenced by tourism and other factors. In order to estimate the seasonal influences better, this is examined in a further sensitivity analysis. In a third sensitivity analysis, the influence of the weekend and the changes in traffic volume at the weekend in the different seasons are examined.

4.2.1 Influence of the number of vehicles

In order to evaluate the influence of the vehicles under consideration, an initial sensitivity analysis is carried out. For this purpose, the input data is increased in two steps. The number of vehicles is increased by the same factor as the expanded fast-charging infrastructure.

1. Multiplication of the input data by a factor of 5
2. Multiplication of the input data by a factor of 10

This results in the following vehicle numbers over 24 hours and the following total capacity along the A2 highway:

	Amount of vehicles over 24h	**Amout of total charging capacity**
Case Study	293	10,355 kW
Case Study × 5	1465	51,775 kW
Case Study × 10	2930	103,550 kW

Table 4.1: Amount of vehicles over 24 hours and amount of the total charging capacity for three different scenarios

The optimizations are repeated with the new input data to analyze the influence of the amount of total vehicles observed. First, the 202 different fleet input and segment input files for both extensions are generated. Figure 4.5 illustrates the three different scenarios. The maximum possible capacity saving as a percentage of the total capacity is plotted as a function of the charging coordination distribution to illustrate the respective savings potential. In this way, the different cases can be compared despite different capacities along the route. The results of the case study are shown in blue, the multiplication by 5 in orange and the multiplication by 10 in green.

The analysis of the data shows that increasing the input data by a factor of 5 (orange) already leads to a significant improvement in the steadily increasing objective function. Although smaller outliers are still recognizable, these occur to a much lesser extent than in the case study (blue). A further increase in the input data and, therefore, the number of vehicles by a factor of 10 (green) results in a further improvement. The course of the

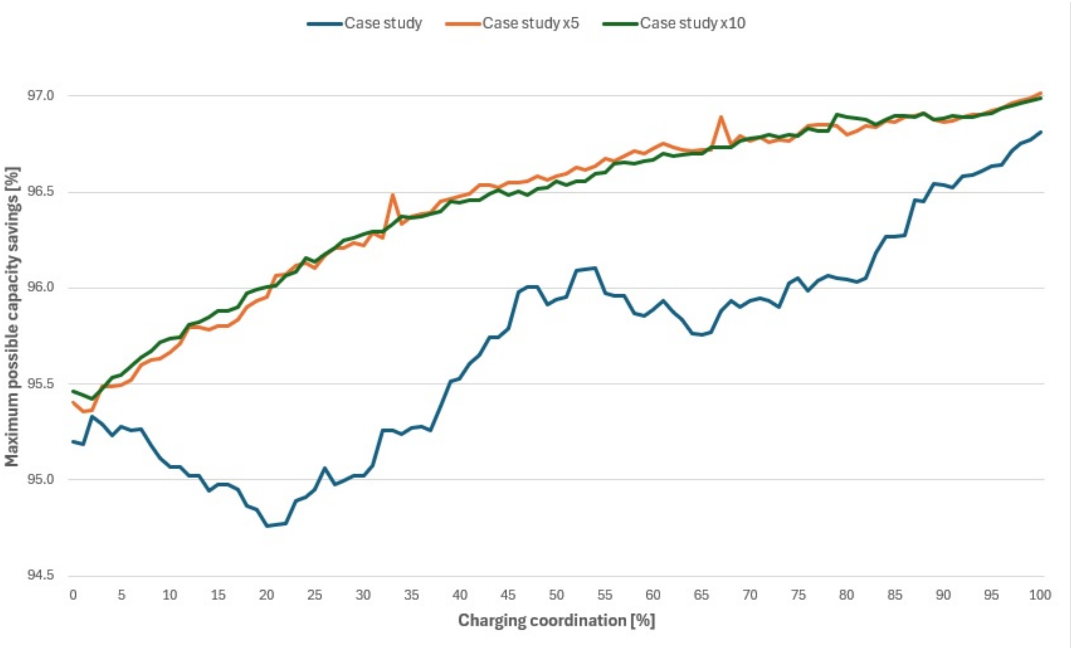

Figure 4.5: Maximum possible capacity savings for the three different scenarios over the different distribution of charging coordination

objective function shows only very slight deviations upwards and downwards and an almost constantly increasing course.

Figure 4.6 illustrates the distribution of charged energy and the respective shares of RND and CTR vehicles over the percentage distribution of charging coordination for scenario case study $\times$ 10. Compared to the distribution of the charged energy in the case study (Figure 4.4), it can be seen that the consideration of a higher number of vehicles significantly smoothes the result. An almost linear decrease in the energy to be charged can be seen as charging coordination increases.

The number of vehicles included in the analysis affects the distribution of charged energy and the measured impact of charging coordination. Figure 4.5 presents the capacity savings achieved through charging coordination compared to a scenario without coordination, showing a difference of up to 1.5 percent.

4.2.2 Influence of the season-related variations in travel patterns

The seasonal influence on capacity savings will be examined in more detail in the following sensitivity analysis. The traffic data, along with the fleets and routes, can

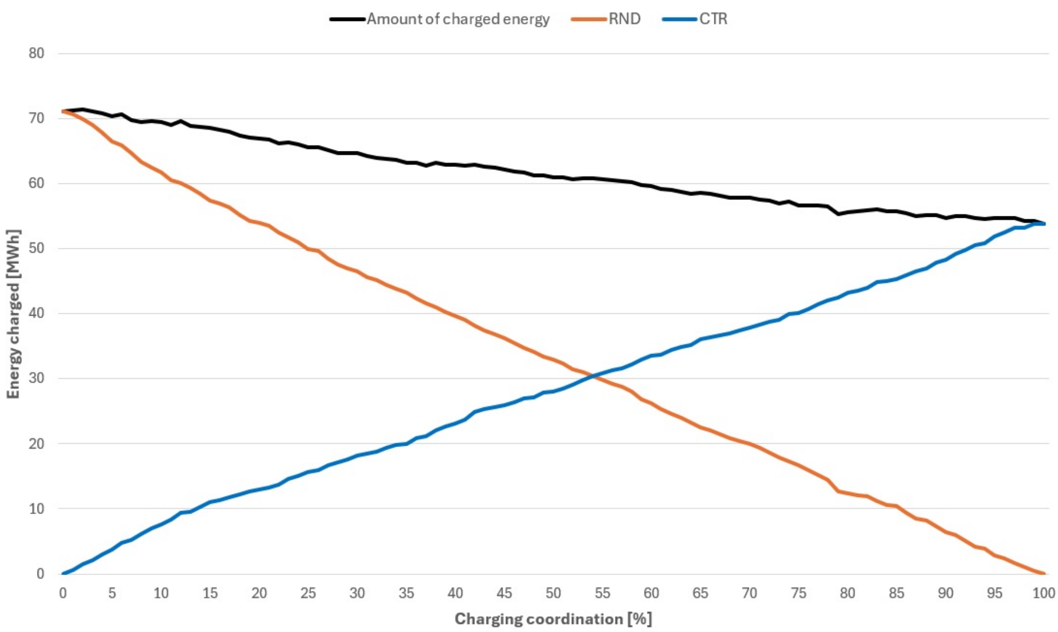

Figure 4.6: Total charged energy for scenario case study × 10 and the distribution between the two categories over the different percentage distributions of the charging coordination share

vary significantly depending on the season. On the one hand, tourism, for example, changes the volume of traffic in Austria at different times of the year. In winter, winter sports, and in summer, vacation traffic in and through Austria plays a significant role in the volume of traffic. In addition, BEVs differ in consumption from winter to summer. In winter, an BEV travels around a quarter less than in summer, due to the higher consumption in winter [42].

In the presented case study the annual counting statistics are used to create the vehicle and route movements, while average values for battery capacity, initial SOC, and specific consumption are used for the vehicle parametrization. In the following sensitivity analysis, a distinction is made between the average year Ø 2023, winter, and summer. The ASFINAG monthly statistics for January 2023 reflect the fleet data for the winter period, while the July monthly statistics are used for the summer period. The counting data values are then re-evaluated to form new total vehicles over 24 hours and new route distributions for the respective season. In addition, a higher specific consumption per 100 km is used for winter and a lower one for summer. The new data is shown in Table 4.2. The average consumption in kW per vehicle on the respective route is also given.

The number of vehicles varies significantly throughout the year. For example, the

Season	Number of vehicles per 24h	Specific consumption (kWh/100km)	Ø Consumption per vehicle (kW)
Ø 2023	293	20	49.7
Winter	255	22.5	56.8
Summer	498	18	46.6

Table 4.2: Overview of the different seasons and the number of vehicles, the specific consumption and the average total consumption of each vehicle over its entire route

number of vehicles in January (winter) is almost twice as high as in July (summer). However, the energy consumption of the vehicles is higher in winter (56.8 kW) compared to summer (46.6 kW). This discrepancy is due to the significantly higher specific energy consumption per 100 km in winter (22.5 kWh/100 km) compared to summer (18 kWh/100 km).

In this sensitivity analysis, the input data is recalculated with a factor of 10, as this has proven to be a more meaningful basis. However,in the following results only four different distributions of charging coordination are optimized as reference points, and a complete objective function is derived from these four optimizations. The four reference points include 0 percent, 20 percent, 50 percent, and 100 percent charging coordination. Figure 4.7 illustrates the unused capacities for the three seasons on the different distributions of charging coordination. The scenario "Case study $\times$ 10" includes an expansion of 103.550 MW capacity.

The analysis of the data shows that the two extreme seasons, winter and summer, reduce the potential capacity and cost savings. The high number of vehicles in summer leads to a reduction in unused capacity despite the lower consumption. The high consumption in winter, in turn, leads to a reduction in potential savings despite the lower number of vehicles. In addition, a convergence of the lines in the different seasons can be seen as charging coordination increases. This leads to the conclusion that charging coordination helps to better balance the different loads caused by the different seasons and increase the savings potential.

4.2.3 Influence of the weekend travel patterns

The case study considers an average day, as described in Subsubsection 3.3.3. The average day covers all days from Monday to Sunday and results in an average. The following sensitivity analysis focuses on the influence of the weekend. The weekend shows significant differences from the weekdays, as it is generally used by most of the population for travel or visits and not for commuting. In the following sensitivity

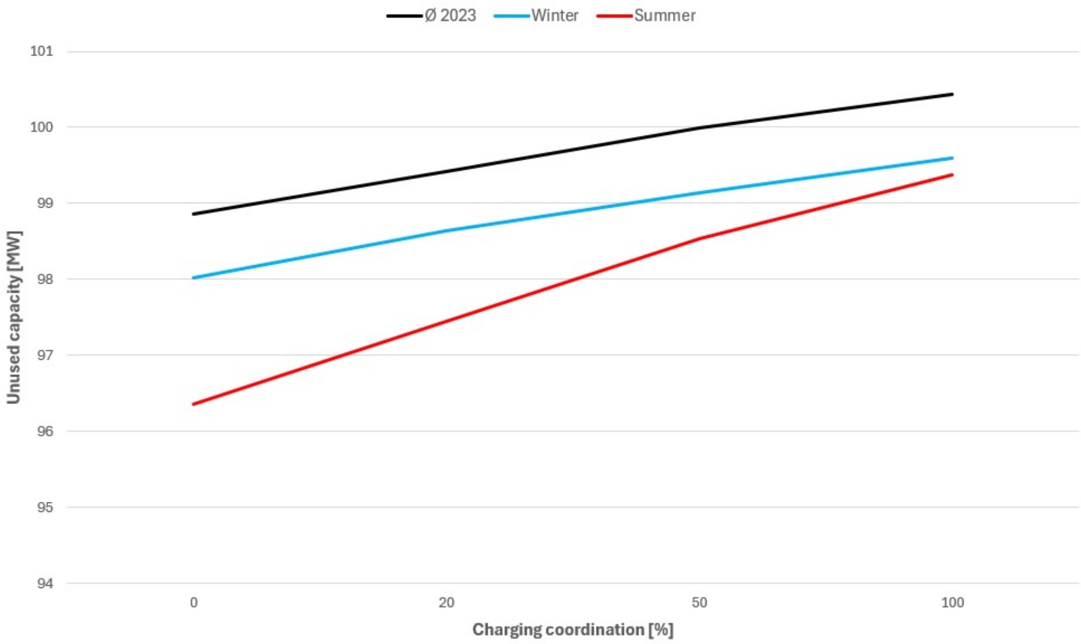

Figure 4.7: Unused capacities in MW in the different seasons with four different distributions of charging coordination and following completion of the objective function

analysis, a distinction is made between average days and weekends for the three previously considered seasons, resulting in new values for the vehicles considered in the various scenarios shown in Table 4.3.

The data analysis shows that, in addition to the number of vehicles, the average consumption per vehicle also changes. This change is due to the adjustment of the vehicle distribution on the various routes, which was determined by the counting point data. On winter weekends, for example, fewer vehicles are on the road, but an average longer distance is traveled. On summer weekends, on the other hand, a higher number of vehicles are on the road, but on shorter routes. Figure 4.8 and Figure 4.9 illustrate the percentage capacity saving in relation to total capacity. The already known possible capacity saving from the previous sensitivity analysis is shown on the left. The possible capacity saving for the weekend is shown on the same scale on the right.

Average day (Monday - Sunday)

Season	Number of vehiclesh per 24h	Specific consumption (kWh/100km)	Ø Consumption per vehicle (kW)
Ø 2023	293	20	49.7
Winter	255	22.5	56.8
Summer	498	18	46.6

Weekend (Saturday - Sunday)

Season	Number of vehiclesh per 24h	Specific consumption (kWh/100km)	Ø Consumption per vehicle (kW)
Ø 2023	361	20	51.7
Winter	223	22.5	58.5
Summer	631	18	46.2

Table 4.3: Overview of the different seasons and the number of vehicles, the specific consumption and the average total consumption of each vehicle on its entire route for an average day and weekend

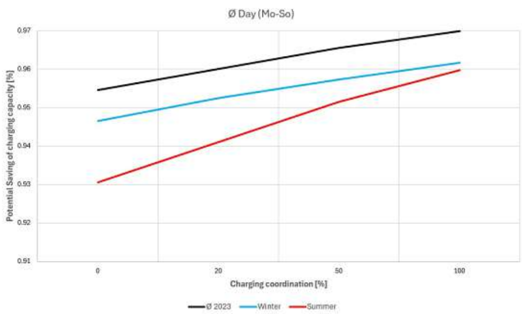

Figure 4.8: Potential savings of charging capacity for average days with four different distributions of charging coordination and following completion of the objective function

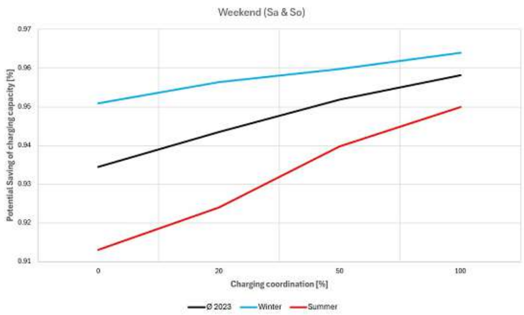

Figure 4.9: Potential savings of charging capacity for weekend days with four different distributions of charging coordination and following completion of the objective function

The results show that, on average over the year and in summer, charging capacity requirements are higher at weekends and, the savings potential is therefore lower. In winter, the capacity requirement is lower, which leads to a marginally higher savings potential. At weekends, a similar phenomenon manifests itself, which was already evident in the results for the average day. The results show that increased coordination of the charging process leads to capacity savings and that extreme fluctuations, such as those caused by the season or the weekend, can be reduced in their impact on the required charging capacities. The difference in the required capacity in relation to the total capacity is 1.75 percent between the average day and the weekend in summer without charging coordination. With charging coordination, this difference is reduced to just 1 percent.

A weekend scenario with 20 percent charging coordination is considered in the following. The maximum utilization rates of all seven segments equipped with a charging station (see Table 3.6) are shown as a percentage of the total capacity. The maximum utilization refers to the time at which the highest capacity requirement exists and, at the same time, the least unused capacity is available. It should be noted that this maximum utilization can occur at a different time step for each segment.

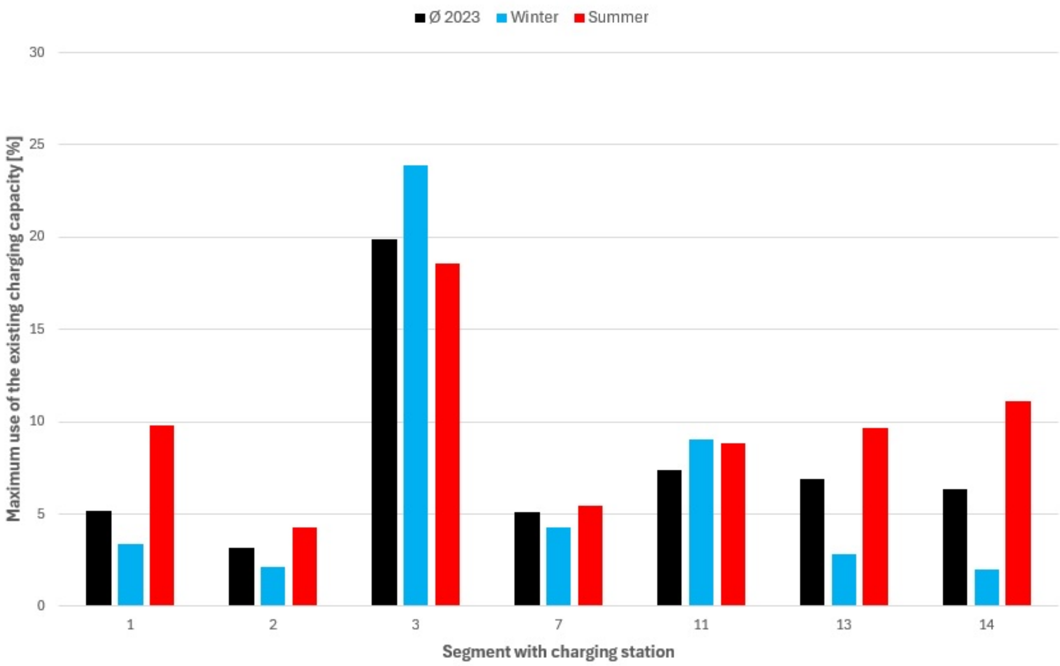

Figure 4.10: Maximum utilization, during the highest usage over all time steps, in percent for the charging stations in the segments containing a charging station for 20 percent charging coordination for the average year 2023, winter and summer on a weekend day

It can be seen that the charging stations located in the middle of the A2 highway (segments 7 and 11) are used by a significantly higher volume of traffic than the charging stations at the ends of the route (segments 1, 2, 3, 13, and 14). The required capacity at the busy charging stations shows less variability than at the peripheral charging stations despite the different traffic volumes between the seasons. In this model, vehicles use peripheral charging stations less intensively than the central charging stations. Segment 7, for example, is crossed by each of the ten existing routes, while segment 14 is only crossed by four routes. The charging station in segment 7 requires only 1.17 percent more fast charging capacity in summer than in winter. In a less busy segment (segment 14), on the other hand, 9.07 percent more fast-charging capacity is required in summer than in winter.The charging power required over all time steps for the CS in segment 7 is shown in Figure 4.11. For comparison, Figure 4.12 shows the charging power required over all time steps for the CS in segment 14.

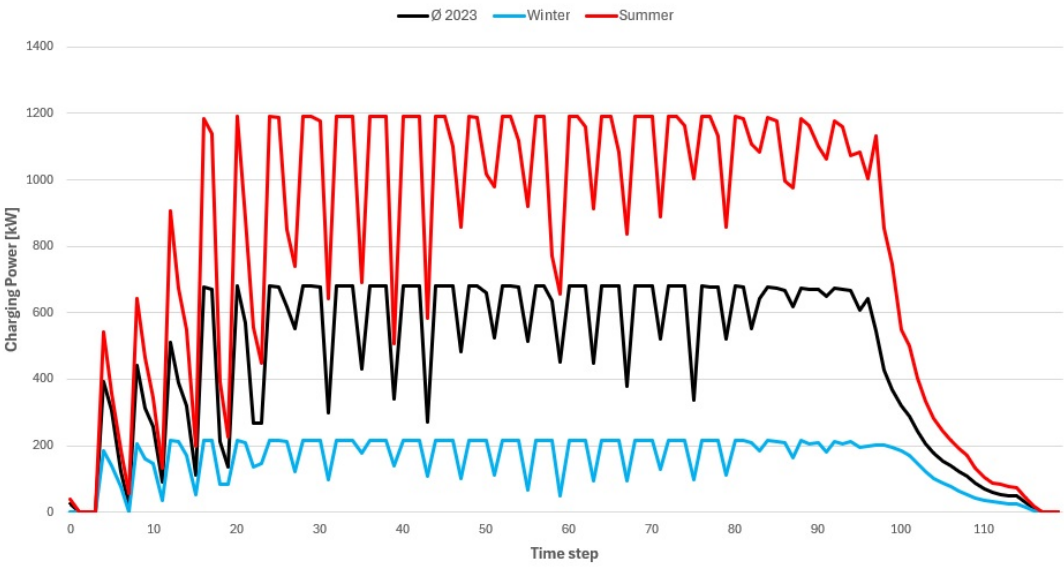

Figure 4.11: Charging power in kW of the charging station in segment 14 over all time steps for three different seasons

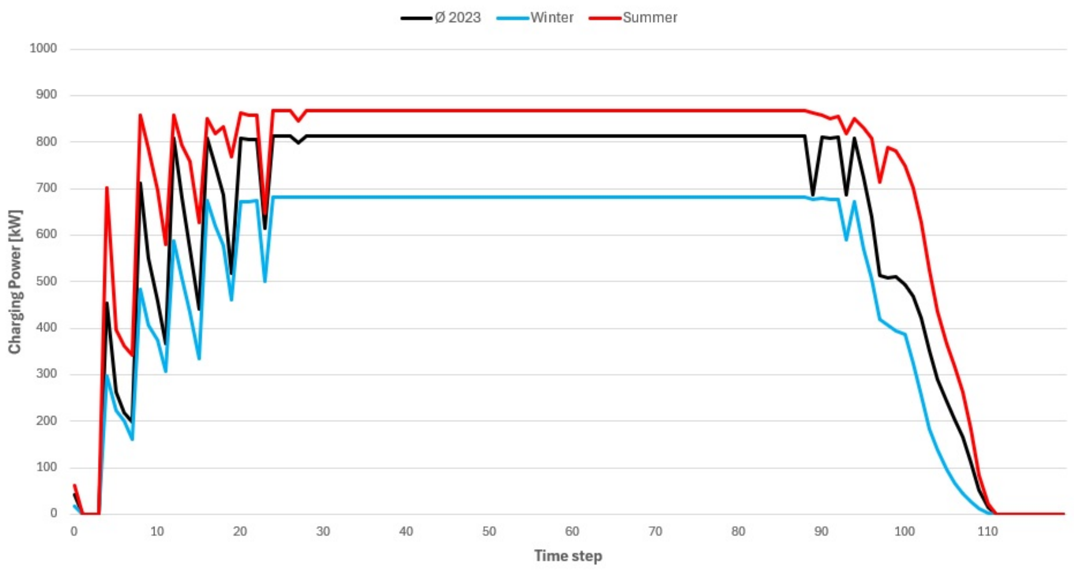

Figure 4.12: Charging power in kW of the charging station in segment 7 over all time steps for three different seasons

The departures in the model shown in Figure 3.7 in the methodology chapter are distributed over 24 hours. It can be seen that a significant number of vehicles are only on the highway network from the sixth hour onwards (corresponds to time step 24). The high number of departures occurs until around 8 p.m. (corresponds to time step 80). Afterward, the vehicles that have just started driving their route. Figure 4.11, which reflects the charging power in segment 7, shows that an almost constant charging power is required during the high amount of departures period (time steps 24 to 80 and slightly beyond). It should be noted that vehicles in the model only depart every 4 time steps. Due to the high number of vehicles passing through segment 7, the charging power can also be distributed constantly over the period in the time steps in which no departures are performed for all seasons. In segment 14, shown in Figure 4.12, the various departures can be seen every 4 time steps. As only a few vehicles pass through this segment, there are temporary drops in the required charging power. This phenomenon manifests itself in both figures for all three seasons investigated. The previous findings indicate that the coordination of the charging process depends on the number of vehicles examined. In addition, optimized coordination of the charging process can help to make more efficient use of the available capacity and to make utilization more even throughout the day. This can lead to avoiding power peaks and promoting charging processes at times of low utilization.

4.3 Utilization of the charging stations

In a final investigation, the influence of charging coordination will be illustrated using one specific segment with CS. For this purpose, the CS in segment 7 is used again, as it is the only one passed by all vehicles. Two optimizations are carried out with identical input data. In one optimization, all vehicles are assigned to the RND category so that no charging coordination occurs. This case is shown in black in Figure 4.13, while full charging coordination (green) assigns all vehicles to the CTR category. The case study is again given a factor of 10 to illustrate the effect of the even distribution of charging power in a busy charging station as observed in Subsection 4.2.3. The analysis of charging coordination shows that a reduction in the required power in this segment of more than 200 kW is achieved compared to optimization without charging coordination. In addition, the required charging power can be kept almost constant over a longer period, leading to a significant reduction in power fluctuations.

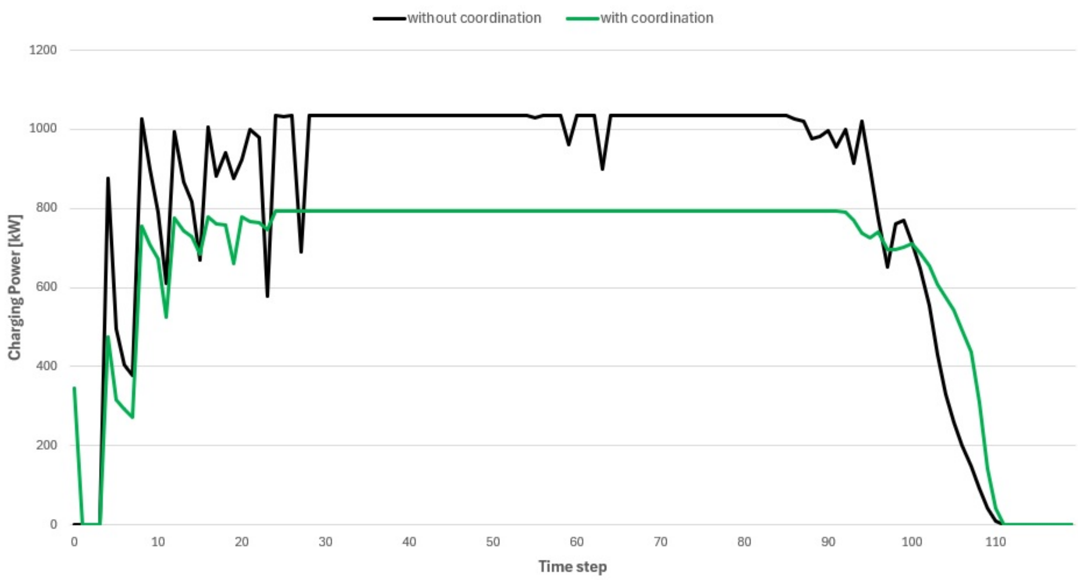

Figure 4.13: Charging power in kW of the charging station in segment 7 over all time steps for full charging coordination and without charging coordination

5 Conclusion and further work

This chapter presents the conclusions obtained and answers the research questions. The applicability of the model in reality, the identified potential for improvement and the charging coordination are evaluated. Finally, suggestions for the further development and expansion of the work and the model are presented.

5.1 Savings potential through charging coordination along an Austrian motorway

In this study, the existing work from Golab et al. [20] was continued and extended to include variable charging coordination. For this purpose, two different vehicle categories were defined, and the behavior in charging duration, charging quantity, and charging time was parameterized based on the SOC of the BEVs at the time of movement. According to this vehicle category classification, vehicles involved in charging coordination have a wider window for initiating the charging process. In addition, a minimum charging quantity has been avoided. These factors allow the charging coordination to react to the charging behavior of the RND vehicles. Furthermore, it was specified that no queues could form at the charging stations in order to prevent the optimization from creating a queue at every charging station and to keep the required capacities low. To finalize the optimization model, fleet movements were established using traffic count data, and cell segments were developed based on highway profiles.

This study confirms the findings of Golab et al. [20] that the installed capacities are oversized. Without charging coordination, capacity savings of 95.2 percent of the total charging capacity along the A2 would be possible. With this saving, all charging processes would be possible without waiting times. These savings can be further increased by introducing charging coordination. With complete charging coordination of all BEVs on the A2, a capacity saving of 96.8 percent would be possible. It is clear that the introduction of charging coordination could further reduce the required capacities. Another positive aspect is that vehicles that are part of this coordination can maintain and distribute the utilisation of the various charging stations more evenly. This has the great advantage that the charging capacities can be better distributed locally. This means that locally high charging demand can be averted and distributed to other charging stations that are currently underutilised.

The increase in the number of BEVs travelling within 24 hours and the expanded fast-charging infrastructure by a factor of 5 and 10 respectively led to the finding that the number of vehicles examined has a significant influence on the more stable relative growth of the available capacity. This effect also extends to the linearisation of the behaviour of the potential capacity savings with different percentage distributions of charging coordination. Increasing the number of vehicles results in an almost constant increase in the influence of charging coordination on capacity savings and the associated cost savings. Furthermore, charging coordination contributes to a better distribution of charged energy, which would help make more accurate forecasts. Increasing the number of vehicles under consideration increases the potential for charging coordination. The increased number of vehicles can compensate for capacity differences even more effectively and ensures an even capacity requirement locally. Assuming a further increase in the share of BEVs in Austria in the future, these effecst could be further strengthened.

The volume of traffic and the routes driven are affected by seasonal fluctuations, which impact the number of routes driven and the drivers' destinations. For example, people travel to different destinations in summer than in winter. In order to evaluate the effects of these seasonal changes on the means of transport, seasonal changes were also examined in this study. The different demands on fleet movements change the required capacity in terms of quantity and local distribution. Charging coordination makes it possible to balance extreme requirements better and to distribute the required capacities better so that the required amount of capacity no longer deviates too much from one another. For example, on an average day in summer without charging coordination, 1.6 percent more of the total fast-charging capacity is required than on an average day in winter without charging coordination. With charging coordination, only 0.2 percent more of the total fast-charging capacity is required in summer than in winter, even though almost double the amount of vehicles are on the road within 24 hours in summer.

This study further analyses traffic changes on weekends at different seasons. In this context, charging coordination also makes it possible to approximate the required capacity differences and confirms the previous findings. In addition, charging coordination helps to equalize the required capacity at locations with high BEV traffic throughout the day, regardless of the season.

5.2 Realisation of charging coordination

This study deals with the idea of charging coordination for BEVs. A key aspect of such coordination would be the obligation of participating vehicles to comply strictly with the specified charging instructions. This implies that the time, duration, and location of the charging process are not freely selectable. In order to promote the acceptance of such restrictions, it would be advisable to provide specific benefits or promises for participating drivers. These could be discounts on the kilowatt hours charged, discounts at neighboring catering establishments, or guaranteeing a secure and prompt charging process. Operators of fast-charging stations could also benefit. A faster return on investment could be achieved through maximised use and optimised utilisation of charging capacities. However, it is also necessary to discuss penalties if the charging coordination requirements are not met. Effective communication between the driver and the charging coordination system is essential. This includes information regarding the driver's destination, journey duration, and preferred rest areas. The suitability of charging coordination is limited to vehicles travelling long distances. In addition, charging coordination must be able to react to short-term changes, which requires real-time adaptation. The introduction of charging coordination makes it possible to precisely analyse the fast-charging infrastructure by identifying overdimensioning and potential bottlenecks in charging capacity. This allows the planning of future expansion projects to be optimised, leading to a significant reduction in peak loads in the system and cost savings.

5.3 Further work and outlook

In this work, the entire time horizon is optimised at once. The model could be extended by creating a "real-time capable" model. Instead of an optimization as "perfect foresight", the model could be extended by optimization with a "rolling horizon". It should also be noted that only one Austrian highway was considered in this work. Extending the input data to the entire Austrian highway network would make it possible to estimate the savings potential throughout Austria. In addition, the model could also be expanded in terms of the accuracy of fleet movements if the segments were extended. In addition, more in-depth analyses of BEV movements on Austrian highways and their departure times could be developed.

Bibliography

[1] C. Corinaldesi, G. Lettner, D. Schwabeneder, A. Ajanovic, and H. Auer, “Impact of Different Charging Strategies for Electric Vehicles in an Austrian Office Site,” en, *Energies*, vol. 13, no. 22, p. 5858, Nov. 2020, ISSN: 1996-1073. DOI: 10.3390/en13225858. [Online]. Available: https://www.mdpi.com/1996-1073/13/22/5858 (visited on 02/12/2025) (cit. on pp. 1, 5).

[2] *The Paris Agreement — UNFCCC (United Nations Framework Convention on Climate Change)*. [Online]. Available: https://unfccc.int/process-and-meetings/the-paris-agreement (visited on 02/01/2025) (cit. on pp. 1, 3, 8).

[3] European Parliament, “Greenhouse gas emissions by country and sector (infographic),” de, Dec. 2024. [Online]. Available: https://www.europarl.europa.eu/pdfs/news/expert/2018/3/story/20180301STO98928/20180301STO98928_en.pdf (visited on 02/01/2025) (cit. on pp. 1, 3).

[4] *Treibhausgase*, de. [Online]. Available: https://www.umweltbundesamt.at/klima/treibhausgase (visited on 02/12/2025) (cit. on pp. 1, 3).

[5] BEÖ - Bundesverband Elektromobilität Österreich, *Österreich: E-Mobilität in Zahlen*, de-DE, Sep. 2024. [Online]. Available: https://www.beoe.at/statistik/ (visited on 09/11/2024) (cit. on pp. 1, 3, 4, 27, 32).

[6] Statista, *Elektrofahrzeuge - Weltweit — Statista Marktprognose*, de. [Online]. Available: https://de.statista.com/outlook/mmo/elektrofahrzeuge/weltweit (visited on 02/01/2025) (cit. on p. 1).

[7] M. Faraj and O. Basir, “Range anxiety reduction in battery-powered vehicles,” in *2016 IEEE Transportation Electrification Conference and Expo (ITEC)*, Jun. 2016, pp. 1–6. DOI: 10.1109/ITEC.2016.7520190. [Online]. Available: https://ieeexplore.ieee.org/document/7520190 (visited on 01/26/2025) (cit. on pp. 2, 18).

[8] *E-Mobilität: Sind unsere Netze stabil genug? — EnBW*, de. [Online]. Available: https://www.enbw.com/unternehmen/themen/elektromobilitaet/e-mobilitaet-sind-unsere-netze-stabil-genug.html (visited on 02/16/2025) (cit. on p. 2).

[9] Statista, *Einwohnerzahlen in Europa nach Ländern bis 2100*, de. [Online]. Available: https://de.statista.com/statistik/daten/studie/164004/umfrage/prognostizierte-bevoelkerungsentwicklung-in-den-laendern-der-eu/ (visited on 02/15/2025) (cit. on p. 3).

[10] *Verkehr beeinflusst das Klima*, de. [Online]. Available: https://www.umweltbundesamt.at/umweltthemen/mobilitaet/mobilitaetsdaten/verkehr-treibhausgase (visited on 02/15/2025) (cit. on p. 3).

[11] *Kfz-Bestand*, de-AT. [Online]. Available: https://www.statistik.at/statistiken/tourismus-und-verkehr/fahrzeuge/kfz-bestand (visited on 02/15/2025) (cit. on p. 3).

[12] Statista, *Österreich - Bestand an Elektroautos 2023*, de. [Online]. Available: https://de.statista.com/statistik/daten/studie/688843/umfrage/elektro-pkw-in-oesterreich/ (visited on 02/15/2025) (cit. on p. 3).

[13] A. Priessner, R. Sposato, and N. Hampl, "Predictors of electric vehicle adoption: An analysis of potential electric vehicle drivers in Austria," *Energy Policy*, vol. 122, pp. 701–714, Nov. 2018, ISSN: 0301-4215. DOI: 10.1016/j.enpol.2018.07.058. [Online]. Available: https://www.sciencedirect.com/science/article/pii/S0301421518305044 (visited on 02/15/2025) (cit. on p. 4).

[14] *Öffentliche E-Ladesäulen in österreich » nach Bundesländern*, de. [Online]. Available: https://positionen.wienenergie.at/grafiken/oeffentliche-e-ladestellen-in-oesterreich/ (visited on 02/15/2025) (cit. on p. 4).

[15] Pfaffenbichler, Paul, "Hochlaufzahlen E-Autos und Bedarf öffentlicher Ladestationen in Wien bis 2040," Tech. Rep., 2022. [Online]. Available: https://positionen.wienenergie.at/wp-content/uploads/2019/10/Hochlaufstudie-Ladestationen_2040_Kurzfassung_final.pdf (visited on 02/15/2025) (cit. on p. 4).

[16] I. Ullah, K. Liu, S. B. Layeb, A. Severino, and A. Jamal, "Optimal Deployment of Electric Vehicles' Fast-Charging Stations," en, *Journal of Advanced Transportation*, vol. 2023, no. 1, p. 6 103 796, 2023, ISSN: 2042-3195. DOI: 10.1155/2023/6103796. [Online]. Available: https://onlinelibrary.wiley.com/doi/abs/10.1155/2023/6103796 (visited on 02/16/2025) (cit. on p. 5).

[17] C. Diaz-Londono, G. Gruosso, P. Maffezzoni, and L. Daniel, "Coordination Strategies for Electric Vehicle Chargers Integration in Electrical Grids," in *2022 IEEE Vehicle Power and Propulsion Conference (VPPC)*, ISSN: 1938-8756, Nov. 2022, pp. 1–6. DOI: 10.1109/VPPC55846.2022.10003274. [Online]. Available: https://ieeexplore.ieee.org/document/10003274 (visited on 02/15/2025) (cit. on p. 5).

[18] T. Faghihi, S. Sabzi, and L. Vajta, "Energy Management Strategy based Charging Coordination for Electric Vehicle Integrated Distribution Grid," in *2023 International Conference on Future Energy Solutions (FES)*, Jun. 2023, pp. 1–6. DOI: 10.1109/FES57669.2023.10182883. [Online]. Available: https://ieeexplore.ieee.org/document/10182883 (visited on 02/16/2025) (cit. on p. 5).

[19] F. Verbist, N. K. Panda, P. P. Vergara, and P. Palensky, *Impact of Dynamic Tariffs for Smart EV Charging on LV Distribution Network Operation*, arXiv:2306.10775 [eess], Jun. 2023. DOI: 0.1109/PESGM52003.2023.10252603. [Online]. Available: http://arxiv.org/abs/2306.10775 (visited on 02/16/2025) (cit. on p. 6).

[20] A. Golab, S. Zwickl-Bernhard, T. Perger, and H. Auer, "Spatio-temporal charging model for the identification of bottlenecks in planned highway charging infrastructure for passenger BEVs," en, *e & i Elektrotechnik und Informationstechnik*, vol. 139, no. 8, pp. 693–711, Dec. 2022, ISSN: 0932-383X, 1613-7620. DOI: 10.1007/s00502-022-01074-5. [Online]. Available: https://link.springer.com/10.1007/s00502-022-01074-5 (visited on 11/10/2023) (cit. on pp. 6–9, 13, 32, 45).

[21] A. Golab, S. Zwickl-Bernhard, and H. Auer, "Minimum-Cost Fast-Charging Infrastructure Planning for Electric Vehicles along the Austrian High-Level Road Network," en, *Energies*, vol. 15, no. 6, p. 2147, Mar. 2022, ISSN: 1996-1073. DOI: 10.3390/en15062147. [Online]. Available: https://www.mdpi.com/1996-1073/15/6/2147 (visited on 01/03/2024) (cit. on p. 8).

[22] Bundesministerium für Klimaschutz, Umwelt, Energie, Mobilität, Innovation und Technologie, *Das übereinkommen von Paris*, de. [Online]. Available: https://www.oesterreich.gv.at/themen/umwelt_und_klima/klima_und_umweltschutz/1/Seite.1000325.html (visited on 12/21/2024) (cit. on p. 8).

[23] *Virta International GmbH - DC Ladestation – Kosten, Lieferzeiten & ideale Einsatzorte*, de, Oct. 2023. [Online]. Available: https://www.virta.global/de/blog/dc-ladestation-kosten-lieferzeiten-ideale-einsatzorte (visited on 09/17/2024) (cit. on p. 12).

[24] *Python*, en. [Online]. Available: https://www.python.org/ (visited on 10/29/2024) (cit. on p. 22).

[25] *Anaconda — Built to Advance Open Source AI*, en-US. [Online]. Available: https://www.anaconda.com/ (visited on 02/01/2025) (cit. on p. 22).

[26] *PyCharm: Die Python-IDE für Data Science und Webentwicklung*, de. [Online]. Available: https://www.jetbrains.com/de-de/pycharm/ (visited on 02/01/2025) (cit. on p. 22).

[27] *Pyomo*, en. [Online]. Available: http://www.pyomo.org (visited on 10/29/2024) (cit. on p. 22).

[28] *Pandas - Python Data Analysis Library*. [Online]. Available: https://pandas.pydata.org/ (visited on 02/01/2025) (cit. on p. 22).

[29] *NumPy*. [Online]. Available: https://numpy.org/ (visited on 02/01/2025) (cit. on p. 22).

[30] *Gurobi*, en. [Online]. Available: https://www.gurobi.com/ (visited on 10/29/2024) (cit. on p. 22).

[31] *FCC Austria sorgt für Sauberkeit auf der A2*, de, Jan. 2018. [Online]. Available: https://www.fcc-group.eu/osterreich/news-media/news/fcc-austria-sorgt-fur-sauberkeit-auf-der-a2 (visited on 09/17/2024) (cit. on p. 25).

[32] A. Wagner, *Karte der österreichischen A2 / Map of austrian freeway A2*, Sep. 2009. [Online]. Available: https://commons.wikimedia.org/wiki/File:Karte_A2_AT.svg (visited on 01/26/2025) (cit. on p. 25).

[33] Bundesministerium für Klimaschutz, Umwelt, Energie, Mobilität, Innovation und Technologie, *Höchstgeschwindigkeiten*, de. [Online]. Available: https://www.oesterreich.gv.at/themen/mobilitaet/kfz/10/Seite.063300.html (visited on 12/21/2024) (cit. on p. 25).

[34] ASFiNAG, *Rastanlagensuche*, de. [Online]. Available: https://www.asfinag.at/parken-rasten/rastanlagensuche/ (visited on 10/03/2024) (cit. on p. 26).

[35] ASFiNAG, *Verkehrsentwicklung*, de. [Online]. Available: https://www.asfinag.at/verkehr-sicherheit/verkehrszaehlung/ (visited on 08/01/2024) (cit. on pp. 26, 27).

[36] ASFiNAG, *Basiskarte*, de. [Online]. Available: https://www.asfinag.at/media/5epp0euq/sondertransport-basiskarte-asfinag-streckennetz-januar-2019.pdf (visited on 08/13/2024) (cit. on p. 27).

[37] S. Datla and S. Sharma, "Impact of cold and snow on temporal and spatial variations of highway traffic volumes," *Journal of Transport Geography*, vol. 16, no. 5, pp. 358–372, Sep. 2008, ISSN: 0966-6923. DOI: 10.1016/j.jtrangeo.2007.12.003. [Online]. Available: https://www.sciencedirect.com/science/article/pii/S0966692307001299 (visited on 09/17/2024) (cit. on p. 28).

[38] T. Thomas, W. Weijermars, and E. van Berkum, "Variations in urban traffic volumes," en, 2008 (cit. on p. 28).

[39] ADAC, *Die besten Elektroautos aller Fahrzeugklassen im ADAC Test*, de-DE, Aug. 2024. [Online]. Available: https://www.adac.de/rund-ums-fahrzeug/autokatalog/autotest/beste-elektroautos/ (visited on 11/11/2024) (cit. on p. 29).

[40] ADAC, *So hoch ist die Reichweite wirklich*, de-DE, Aug. 2024. [Online]. Available: https://www.adac.de/rund-ums-fahrzeug/elektromobilitaet/elektroauto/stromverbrauch-elektroautos-adac-test/ (visited on 11/11/2024) (cit. on p. 30).

[41] ADAC, *Elektroauto im Winter: So wirkt sich Kälte auf Verbrauch und Reichweite aus*, de-DE, Jan. 2024. [Online]. Available: https://www.adac.de/rund-ums-fahrzeug/elektromobilitaet/laden/elektroauto-reichweite-winter/ (visited on 11/11/2024) (cit. on p. 35).

[42] Rauecker, Günter and Stich, Christian, *Test Reichweite E-Auto Sommer/Winter — öAMTC*, de-at. [Online]. Available: `https://www.oeamtc.at/autotouring/auto/test-reichweite-e-auto-sommer-winter-62074282` (visited on 11/11/2024) (cit. on p. 37).

Appendix

Appendix A. Directory of resources

Resources	Used for	Where
Grammarly	Spellchecking and correcting the grammatics	Total work
ChatGPT	Creating code samples for plots, help with code issues Creation of textual examples and structures	Total work
Deepl	Help with translation and spellchecking	Total work

Table A1: Directory of resources